Substantia
An International Journal of the History of Chemistry

Firenze University Press
www.fupress.com/substantia

Historical Articles

History of Research on Phospholipid Metabolism and Applications to the Detection, Diagnosis, and Treatment of Cancer

Peter F. Daly[1], Jack S. Cohen[2,*]

[1] *University of Pittsburgh Medical Center, Pittsburgh, PA USA*
[2] *Chemistry Department, Ben Gurion University, Beer Sheva, Israel*
*Corresponding author. Email: cohenjk@post.bgu.ac.il

Abstract. In the past 30 years there has been a significant increase in the number of publications on phospholipid (PL) metabolism, both for the medical purposes of detection and diagnosis of cancer and for the monitoring of the treatment of human cancers. Most of the work has focused on the pathway that produces phosphatidylcholine, the major component of human cell membranes. The trigger for this research was the advent of applications of NMR spectroscopy *in vitro* and *in vivo* in the 1980's and observations that most cancer cells and tumors had significant increases in the water-soluble PL precursors and breakdown products. Increased phosphocholine (PC) has been focused on as a marker for cancer using Magnetic Resonance Spectroscopy (MRS) and Positron Emission Tomography (PET). MRS is now used clinically to aid in the diagnosis and severity of some brain tumors; and choline PET is used for the diagnosis and staging of recurrent prostate cancer, paid for by medical insurance companies. Another major area of research starting in the 1990's was the development of specific choline kinase (CK) inhibitors aimed at the isoenzyme CK-a. This isoenzyme is markedly upregulated in cancer cells and unexpectedly was found to have a role in oncogenic transformation independent of its enzyme function.

Keywords: phospholipid metabolism, phosphocholine, MRS, PET, choline kinase, cancer diagnosis.

Citation: Daly P.F., Cohen J.S. (2022) History of Research on Phospholipid Metabolism and Applications to the Detection, Diagnosis, and Treatment of Cancer. *Substantia* 6(1): 49-76. doi: 10.36253/Substantia-1376

Received: Aug 08, 2021

Revised: Nov 20, 2021

Just Accepted Online: Nov 22, 2021

Published: Mar 07, 2022

Data Availability Statement: All relevant data are within the paper and its Supporting Information files.

Competing Interests: The Author(s) declare(s) no conflict of interest.

* List of Abbreviations used: **^{18}FCH,** ^{18}F-fluorocholine; **Ala**, Alanine; **BCR**, Biochemical Recurrence; **CK**, choline kinase; **CSI,** Chemical Shift Imaging; **CT**, Computed tomography; **DWI**, Diffusion Weighted Imaging; **FDA**, United States Food and Drug Administration; **FDG**, ^{18}F-fluorodeoxyglucose; **Ga-68,** Gallium-68; **GPC**, Glycerophosphocholine; **GPE**, Glycerophosphoethanolamine; **HC-3**, Hemicholinium-3; **HGG**, High grade glioma; **Lac**, Lactate; **mpMRI**, multiparametric MRI; **MRI**, Magnetic resonance imaging; **MRS**, Magnetic resonance spectroscopy; **MRSI**, Magnetic resonance spectroscopic imaging; **NAA**, N-acetyl-aspartate; **NMR**, Nuclear Magnetic Resonance; **PC**, phosphocholine; **PCr**, phosphocreatine; **PDE**, phosphodiester; **PE**, phosphoethanolamine; **PET**, Positron emission tomography; **PL**, phospholipid; **PME**, phosphomonoester; **PSA**, Prostate specific antigen; **PSMA**, prostate specific membrane antigen; **PtdCho**, phosphatidylcholine; **PtdEth**, phosphatidylethanolamine; **tCho**, total choline peak; **tCr**, total creatine peak.

INTRODUCTION

Lecithin was one of the first organic substances described, isolated by the French chemist Theodore Gobley from egg yolk in 1845.[1] The chemical structure of phosphatidylcholine, one of its main components, was not established until 1874.[2] Over the next century much work was done that led to our understanding of the metabolism of the PL components that make up the cell membrane of mammalian cells.[3]

At first PL metabolism in cells and tissues were studied by invasive techniques, such as cell lysis and extracts[4] and freeze-trapping.[5] However, it was eventually realized that these techniques gave unreliable results because of the rapid release of kinases that degraded the substances of interest. It was realized that noninvasive techniques were needed to quantitatively assess the levels of PL metabolites in intact cells and tissues.[6] Foremost among these methods was the use of noninvasive NMR spectroscopy (MRS) to detect phosphate-containing metabolites such as ATP using ^{31}P MRS as first observed by Mildred Cohn in 1960.[7]

Metabolism of intact cells was investigated by ^{31}P MRS using a perfusion technique with cells trapped in a gel[8, 9] and tissues were investigated *in vivo* using specially developed surface detection coils.[10] This included direct investigation of phosphate-containing metabolites in tumors grown on nude mice.[11, 12] These studies resulted in the observation that the levels of PL metabolites such as PC and phosphoethanolamine (PE) are higher in rapidly dividing cells such as cancer cells that are non-contact inhibited than in normal contact-inhibited cells.[13-15] Several authors have identified these studies as the trigger initiating interest in use of these findings in cancer diagnosis and detection.[16-20]

Parallel noninvasive studies were carried out using proton (^{1}H) MRS, but these were more difficult due to the presence of the huge H_2O solvent peak, requiring water-suppression methods.[21] For tissues *in vivo*, because of the greater sensitivity of the method, spatial localization techniques were developed using gradient methodology.[22, 23] Although these MRS methods demonstrated the basic observation that increased cell membrane biosynthesis could be used as a monitor of cancer cells, ^{31}P MRS was too insensitive and initially ^{1}H MRS was too cumbersome to be applied *in vivo* and in the clinic for human applications. A much more sensitive tomographic method was needed and that has become positron emission tomography (PET) that has allowed these research observations to be applied clinically to the detection and diagnosis of cancer.[24, 25] Eventually ^{1}H Magnetic Resonance Spectroscopic Imaging (MRSI) was developed to be more sensitive and less cumbersome and is now used clinically in brain tumors.[26]

Also, as a result of the differences between PL metabolism in cancer and normal cells, it was realized that kinase inhibitors could be effective anti-cancer drugs and this has resulted in the development of potential anti-cancer therapeutics.[27, 28]

PHOSPHOLIPID (PL) METABOLIC PATHWAYS

The two biochemical pathways for the two main components of the PL membrane in humans, PtdCho (phosphatidylcholine) and phosphatidylethanolamine (PtdEth), were worked out by Eugene Patrick Kennedy in 1956[29] and are commonly referred to as the Kennedy pathways (Figure 1).

Research on these two pathways has continued at a steady pace since 1956, but greatly increased starting in the late 1980s due to observations made using NMR Spectroscopy which was being used *in vitro* in cell suspensions and *in vivo* in animal and human tumors. These studies indicated these pathways were more active in cancer cells. The PL membrane makes up 70% of the dry weight of human cells and PtdCho and PtdEth make up to 70% of the lipid portion of the membrane.

The Kennedy Pathways,[31] are relatively simple three step pathways that are completely analogous. Furthermore, choline is trimethylethanolamine and the 3 extra

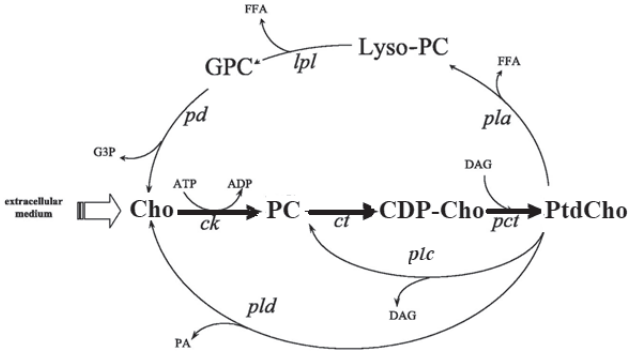

Figure 1. Kennedy pathway (center bold pathway) showing biosynthesis of the main PtdCho component of mammalian cell membranes from PC and the break-down pathway to glycerophosphocholine (GPC). A parallel pathway exists for PtdEth.[30] The enzymes involved in the pathways are shown in italics. Abbreviations: **CDP-Cho**, Cytidine diphosphate-choline; **Cho**, choline; ***ck***, Choline Kinase; ***ct***, Cytidylyltransferase; **DAG**, Diacylglycerol; **FFA**, Free fatty acid; **G3P**, Glyerol-3-phosphate; **GPC**, Glycerophosphocholine; ***lpl***, Lysophospholipase; **Lyso-PC**, Lysophosphocholine; **PA**, Phosphatidic acid; ***pct***, Phosphocholine transferase; ***pd***, Phosphodiesterase; ***pla***, Phospholipase A; ***plc***, Phospholipase C; ***pld***, Phospholipase D.

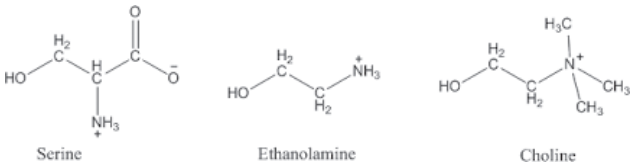

Figure 2. Chemical structures of ethanolamine and choline.

CH3 groups in choline (Figure 2) allow for it to be more easily observed in ^{1}H NMR spectroscopy *in vivo* and *in vitro* since the signal derives from the 9 equivalent H atoms of the trimethylated nitrogen atom.

Most of the research since 1990 has focused on the choline pathways. For the sake of simplicity, we will only show figures of the choline pathways although the ethanolamine pathways are completely analogous.[29]

The simple three step Kennedy pathway[32] for synthesizing phosphatidylcholine is:

Choline to Phosphocholine to CDP-Choline to Phosphatidylcholine.

This is the central synthetic pathway in Figure 1 going from left to right. The degradative pathways occur via the phospholipase A (*pla*), phospholipase C (*plc*), and phospholipase D (*pld*) pathways that are shown above and below the central synthetic pathway in Figure 1 going from right to left.

The metabolites that are seen in ^{31}P MR spectra of *in vitro* cell suspensions and *in vivo* are **PC** in the synthetic phosphatidylcholine pathway; and **PE** in the analogous synthetic PtdEth pathway (not shown) and **GPC** (Glycerophosphocholine) and **GPE** (Glycerophosphoethanolamine) in the degradative pathway starting with phospholipase A (*pla*). The degradative pathway via Phospholipase C (*plc*) contributes a small percentage of the **PC** peak in the NMR spectra.

The degradative pathways have also drawn interest not only because they produce **GPC** and **GPE** which are observed in the ^{31}P NMR spectra of tumors. But the degradative pathways also produce the metabolites phosphatidic acid (PA) via phospholipase D (*pld*); and diacylglycerol (DAG) via phospholipase C (plc) which are second messengers within the cell involved in multiple functions including growth and the mitogenic activity of growth factors via the RAS family of proteins.[33-36] The RAS proteins have enzymatic activity and exist in an "on" and "off" state. When turned on they trigger a cascade that ultimately turns on genes involved in cell growth, differentiation, and survival. Overactive signaling inside the cell can ultimately lead to cancer.[37]

CK is the first enzyme in the Kennedy pathway and has been found to be overproduced in almost all cancers beyond their need for phosphatidylcholine synthesis and has been under intense study in the past 25 years as a key enzyme in cancer and necessary for oncogenic transformation. CK also interacts with the RAS protein family for signal transduction and high concentrations of CK have been noted to turn on RAS proteins for signal transduction.[17, 38] Multiple CK inhibitors have been synthesized as potential chemotherapy agents for cancer.[27] As the first step in the synthetic pathway CK phosphorylates choline to **PC.** The next enzyme in the pathway is cytidylyltransferase (*ct*) which is rate limiting and PC accumulates and is easily seen in ^{31}P MR spectra *in vitro* in cancer cells and *in vivo* in tumors.

APPLICATION OF MRS

In 1980 Jack Cohen joined the National Cancer Institute with the intention of using NMR spectroscopy as a tool to study the metabolism of cancer cells. A Varian 400 MHz NMR spectrometer was purchased, and studies began in 1981. The basis of this work were the attempts made to devise a system whereby this noninvasive NMR technique could be used to study cancer cells *in vitro*. Previous attempts using suspensions of cells had proved unsuccessful, since the large number of cells (ca. 10^{9} cells) in 1 ml in a 10 mm ^{31}P MRS tube required to obtain sufficient signal-to-noise, used up all the available nutrients and became ischemic before any useful results could be obtained.[39]

Our first attempt to overcome this problem was to suspend cancer cells in an agarose gel and attempt to perfuse it with a solution containing nutrients and oxygen.[40] But this was not really successful. In order to enable the cells to metabolize, the solution had to be in contact with all of the cells as much as possible. We then devised a method to place the cell suspension in a liquid gel and flow it through a fine capillary (0.5 mm id) that was dipped in a container of ice, whereupon the mixture gelled and the cells were trapped and the spaghetti-like gel threads were then extruded into an NMR tube and could be perfused with the nutrient-containing and oxygenated solution and remain metabolically active for days[8] (Figures 3-5).

Using this technique we were able to see a high level of ATP in the cells as well as other metabolite signals (Figure 6), and by adding other metabolites or drugs to the solution being pumped through the cells we could monitor changes in the metabolism of the cells.[9, 42]

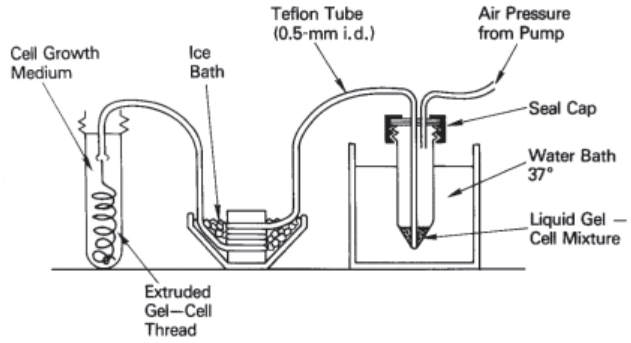

Figure 3. Diagram of the apparatus used to embed cells within agarose gel threads. A mixture of cells in medium is extruded through a fine Teflon capillary in chilled ice. The gel thread is then extruded directly into medium in the 10-mm screw-cap NMR tube.[41]

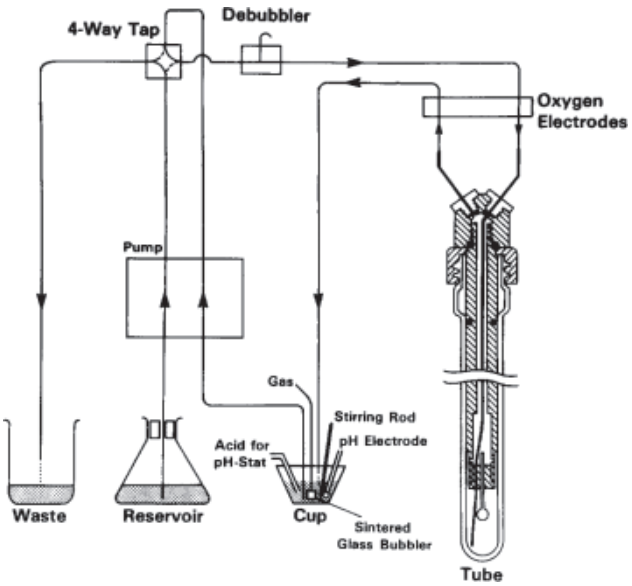

Figure 4. Schematic of the perfusion system showing the arrangement of the polyethylene insert.[41]

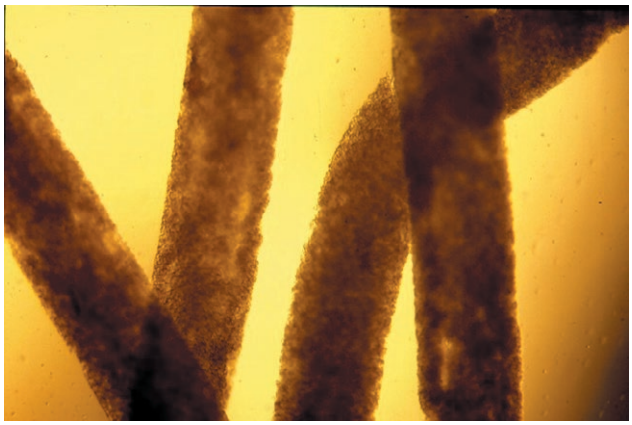

Figure 5. Photomicrograph of gel-threads showing cancer cells embedded in perfusable gel.[41]

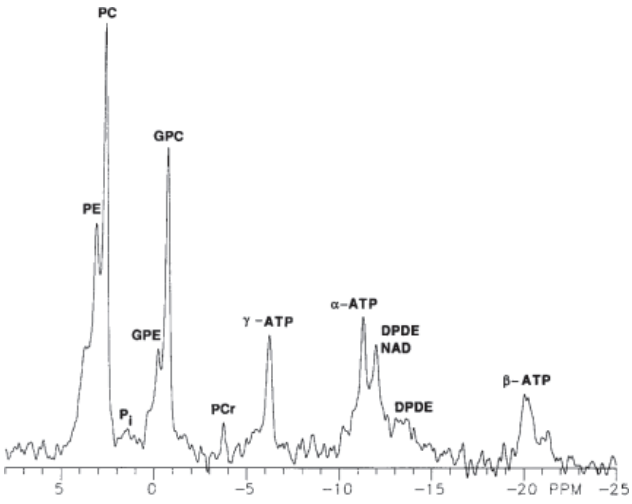

Figure 6. Representative ^{31}P NMR spectrum at 162 MHz of wild-type MCF-7 human breast cancer cells (~10^8/ml) perfused with IMEM media (Pi-free) in agarose gel thread (0.5 mm); 200 scans were accumulated with a recycle time of 40 sec and a 90° pulse. The peak assignments are denoted: PE, PC, Pi, inorganic phosphate; GPE, GPC, PCr, phosphocreatine; ATP, adenosine triphosphate, DPDE, diphosphodiesters; NAD, nicotine adenine dinucleotide.[41]

We carried out a series of studies that resulted in greater understanding of the metabolic response of several cancer cell lines grown in culture under different circumstances. [15,16, 43-46] In earlier studies the phosphomonoester (PME) peaks were erroneously assigned to sugar phosphates (SP), but we confirmed their assignment to PC and PE by the addition of choline and ethanolamine (separately) to the perfusion solution.[13] This was the first observation of the enzymes of the PL pathways functioning in *real time* in *intact cells* by MRS. On addition of ethanolamine, all four peaks, PC, PE, GPC, and GPE reacted to ethanolamine as expected by well-established substrate and inhibition effects. Ethanolamine inhibits CK and the phosphodiesterases that break down GPC and GPE to choline and ethanolamine, and it is the substrate for ethanolamine kinase producing PE. All four peaks can be seen reacting to the ethanolamine infusion as expected in Figure 7.[13]

One of our initial observations was that the peak assigned to PC and PE in the spectrum of cancer cells was found to be higher than expected (Figure 6) and higher than the same peak in *in vivo* studies of normal tissue that were used as controls.[47, 11] This important observation of elevated PC and PE in cancer cells was

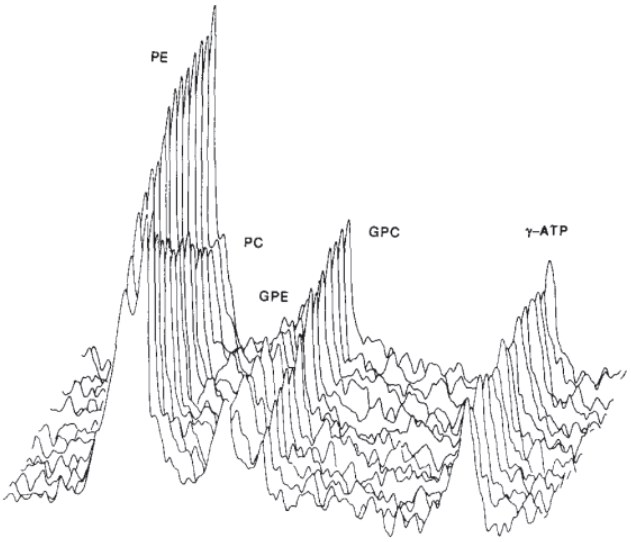

Figure 7. Effect of ethanolamine in the perfusate. Shown are quantitative ^{31}P NMR spectra of cells grown in IMEM medium with 15 mM choline and no ethanolamine, harvested at log phase, and then perfused with Buffer A, 11 mM glucose, plus 2 mM ethanolamine at 37°c. Each spectrum represents a l-hr accumulation. Hours 2 to 16 are shown.[13]

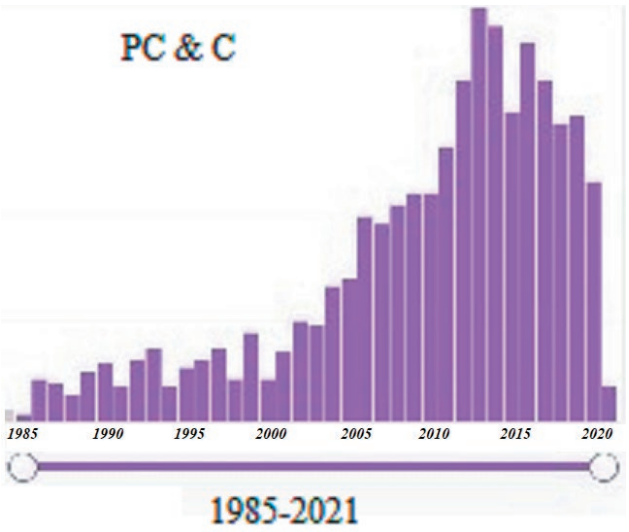

Figure 8. Plot of number of hits vs. year for a search of "phosphocholine and cancer" using the Scifinder (CAS) search engine, with 1,485 hits at maximum..

the basis for many future studies and has had significant influence in subsequent studies of cancer diagnosis and detection. In fact, in several reviews,[17-20] this observation has been singled out as the seminal observation that resulted in much greater research activity in this field (Figure 8). Note that a similar pattern of increase in research activity was found for every topic that was searched in this field.

This observation of increased PC in cancer cells was later confirmed by several authors using as controls noncancerous cells grown in culture.[38, 48] This subject has been extensively reviewed by Glunde and coworkers.[49] in which they document increased PC/PE in 6 different cancer types, including breast,[50, 51] ovarian,[52] prostate,[53, 54] cervical,[55, 52] brain[56, 57] and endometrial[58] cancers. Of significance was the observation of the PME to phosphodiester (PDE) ratio, the more malignant the cell line the more PC and PE were present and the less GPE and GPC were observed. It is this ratio that is more significant, not the absolute concentrations. In the first observation of this type in 1986, comparing the perfused wild-type cell line to the Adriamycin-resistant cell line derived from it, adding up the PME and the PDE concentrations, the wild-type had a PME/PDE ratio of ca. 2, but the resistant more malignant cell line ratio was about 16.[47] Some biochemists looking at choline metabolites call this the PC/GPC "switch" as the malignancy progresses.[38, 30, 19]

We later improved the perfusion technique by using basement gel membrane as the gel substance.[59] Meanwhile others had developed other methods of monitoring the ^{31}P MRS of cells using both suspensions aerated by oxygen[60] and bioreactors.[61, 62] It should also be mentioned that similar perfusion studies were performed with ^{13}C labelled metabolites observed by ^{13}C MRS[63] or by ^{1}H MRS using the ^{13}C-^{1}H spin-spin (J) coupling to gain higher sensitivity.[64, 65] Direct proton MRS studies of choline levels have also been measured.[66]

It should be pointed out that the signals of the PLs themselves are not observed in these ^{31}P spectra of cells, because they are extensively broadened by spin-spin (T2) relaxation due to their macromolecular structure and restricted motion leading to efficient T2 relaxation. By contrast, the metabolites that are smaller molecules with extensive molecular motion, even though within the viscous milieu of the cell, provide narrower resonances. In effect the cellular metabolites provide a ^{31}P MR spectrum that is in fact superimposed on the top of a very broad PL baseline.

DEVELOPMENT OF CHOLINE-PET SCANNING AS A DIAGNOSTIC METHOD FOR PROSTATE CANCER

The observations of the 1980s and their confirmation by further cell studies in the 1990s that the majority of cancer cells had unusually high levels of PC and GPC increased interest in using this fact as a way to diagnose and stage cancer; and to monitor and adjust cancer thera-

py. Since the 1990s the main problem with using MRS for these purposes was the low signal to noise ratio in MRS requiring large "voxels" or cubes of tissue for obtaining a good spectrum. With phosphorus spectra this required voxels that were multiple centimeters in diameter and would sample tissue other than the tumor, including normal tissue and necrotic tissue. ^{1}H spectra using proton MRS was developed and could obtain spectra from 1 cm^{3}. [67, 68, 23] While this was helpful with brain tumors it was still too large a volume for many other common cancers.

To overcome the signal to noise problem ^{11}C-choline for human Positron Emission Tomography (PET) scans was synthesized in 1997 by a Japanese Group led by Hara.[69] Historically, the first synthesis of ^{11}C-choline for PET scans was in 1983 and was used to observe normal brain tissue in a monkey.[70] The Japanese group however used their own synthesis as there were no details for the synthesis given in the 1983 paper. Radiolabeled choline has been used since 1997 in PET in cancer research for imaging brain and other tumors.[69, 71, 72] This is based on the first step in PL synthesis, choline being rapidly metabolized to PC by CK (Figure 1). In addition most cancers have increased membrane transport of choline compared to normal cells.[17]

The two forms of choline most commonly used in PET scanning are ^{11}C-choline and ^{18}F-fluoromethylcholine,[73] which is commonly called ^{18}F-fluorocholine (^{18}FCH). In ^{11}C-choline one of the ^{12}C carbons in the N-trimethyl group of choline (see Figure 2) is replaced by an ^{11}C atom. In ^{18}FCH, one the of the hydrogens in the N-trimethyl group of choline is replaced by ^{18}F. ^{18}FCH was first synthesized by DeGrado in 2000.[74, 75] They found that ^{11}C-choline and ^{18}FCH behaved similarly in cell cultures and also in their ability to be metabolized by CK. Later studies showed that ^{18}FCH was comparable in diagnostic ability to ^{11}C-choline, but is easier to use because of its longer half-life.[76-78] ^{11}C has a half-life of 20 minutes and ^{18}F of 110 minutes allowing for ^{18}FCH PET images to be obtained for a longer time, from 5 min to 60 min after injection. Other choline analogs were synthesized,[74] but these contained additional carbon atoms and were not transported as well by choline membrane transport proteins or metabolized as well by CK.[74]

Since CK is overexpressed in most cancers and rapidly metabolizes choline to PC; most cancers contain higher concentrations of PC compared to normal cells.[79] This generates a visible signal in the PET scanner. From the time ^{11}C-choline and ^{18}FCH were synthesized in 1997 and 2000 it was found that multiple tumors could be found by choline-PET, including brain, head and neck, breast, lung, esophageal, liver, kidney colorectal, prostate, bladder, uterine, ovarian cancers, and lymphomas.[80] For medical use though, it must be shown that it is better than other imaging methods, cost effective, and also has the ability to obtain an image in a time that is comfortable or tolerable for the patient. When PET is combined with a CT or MRI scanner it gives a more accurate location of tumors or metastases.[73] Since 2000 when the PET/CT was first invented most studies have been done with the PET/CT scanner.

The initial studies done from 1997 into the early 2000s showed that ^{11}C-choline or ^{18}FCH did produce clearly delineated images of tumors with a good signal to noise ratio. But for most tumors it was not better than ^{18}F-fluorodeoxyglucose (FDG) PET scans for tumors, which was already in widespread use. FDG works well because it is a glucose analog, and most cancers have a high rate of glucose uptake and utilization. And for brain tumors amino acid PET tracers were also superior.[73] However prostate cancer is an exception in that it is more slowly growing and does not absorb FDG rapidly. In addition, prostate cancer is one of the most common cancers in men with a high mortality rate. It was shown in 2003 that ^{18}FCH PET scans were superior to FDG for restaging prostate cancer after recurrence and this resulted in a marked decrease in the use of FDG for imaging prostate cancer and an increase in choline-PET,[73, 81] both for the initial staging and restaging of prostate cancer after relapse. Unfortunately, in prostate cancer relapse is high so comparative imaging in initial stage and relapse is of utmost importance. Prior to choline-PET tracers, staging was done using CT, MRI images, and ultrasound.

Most of the research on the clinical applications and actual clinical use of choline-PET has occurred in Europe, Japan, and Australia.[24] This is due to the difficulty of getting approval from the FDA (United States Food and Drug Administration) for new PET tracers and financial barriers such as uncertain reimbursement in the USA.[24, 82] ^{11}C-choline was approved by the FDA in 2012 but ^{18}F-choline has not been approved as of 2021, even though it was developed and tested in the USA at Duke University in 2000.[74] After initial studies from 1998 to 2003 showing the feasibility of choline-PET and choline-PET/CT there have been thousands of studies since 2003 focusing on the clinical applications of choline PET. ***The area that it has proven the most useful is in the restaging of relapsed prostate cancer.***

The use of choline PET/CT has become common since about 2010 in many parts of the world for the initial staging and restaging of prostate cancer.[24, 73, 83] A 2021 paper from France started by saying *"F-choline PET/CT is considered a cornerstone in the staging and restaging of patients with prostate cancer."*[84] Another

study published in 2020 focused on the "real world" use of choline-PET showed that it was commonly used for both initial staging and restaging and resulted in a change of therapy in 58% of the patients.[85]

In addition, new PET radiotracers have been developed in the past decade that focus on prostate specific membrane antigen (PSMA) or amino acid tracers such as ^{18}F-FACBC (Fluciclovine) for imaging prostate cancer; and studies are ongoing comparing the effectiveness of each of these tracers compared to ^{11}C-choline or ^{18}FCH.[24] Also, when using choline-PET in patients with prostate cancer, tumors other than prostate cancer are picked up incidentally in 1 to 2 % of patients.[84]

STAGING OF PROSTATE CANCER WITH CHOLINE-PET COMPARED TO MRI

Initial (Primary) Staging; Locating the cancer in the preoperative prostate

Numerous studies were done from 2003 onward evaluating the use of choline-PET scanning for the initial staging of prostate cancer.[73] One study from 2006 focusing on the local detection of prostate cancer nodules by ^{11}C-choline within the prostate preoperatively compared with biopsies done preoperatively[86] did show choline-PET could find 83% of prostate nodules that were 5 mm or greater in diameter, but only 4% of nodules smaller than that for an overall sensitivity of 66% compared to the biopsies. 5 mm is generally considered the lower limit in size detection for PET scans in general -- not just for choline studies.

Another study in 2010[87] looked at the preoperative evaluation of cancer nodules within the prostate as compared to preoperative biopsies, or examination of the prostate by a pathologist after surgical removal. A combination of standard MRI images combined with gadolinium enhanced images of the preoperative prostate found 88% of the nodules, ^{11}C-choline-PET found 73% of the nodules, and FDG-PET found only 31%. Multiparametric MRI (mpMRI) studies in 2015 using DWI (Diffusion Weighted Imaging) showed mpMRI to be superior for detecting cancer in the preoperative prostate as well as local extensions outside the prostate.[88] For modern prostate cancer imaging mpMRI uses four sequences: T1-weighted images, T2-weighted images, DWI, and dynamic contrast enhanced (DCE) imaging. Most commonly T2-weighted images with DWI and DCE are use or T2 weighted images with just DWI. In the past MRS of the prostate was also used as a fifth option to be part of the mpMRI workup but MRS of the prostate is not commonly used currently.

Lymph node and bone metastases

The two other areas of importance in the initial staging are metastases to nearby lymph nodes and bone. Choline-PET/CT was found in many studies to be superior to CT and conventional MRI scans at finding metastases to the lymph node. One reason may be that CT and conventional MRI rely mostly on the size and appearance of the lymph nodes whereas choline PET/CT that has a functional component was able to detect micrometastases to the lymph nodes.[89] The sensitivity of these studies was only about 50% however when compared to the lymph nodes that were removed at the time of surgery and examined by a pathologist.[89, 73] For this reason, The European Association or Urology in 2021[90] still recommends lymph node removal for proper staging of prostate cancer at the time of initial diagnosis. Since PET/CT images the entire body, one important value of choline-PET/CT is that it can detect lymph nodes with prostate cancer outside the area of a standard MRI scan or outside the surgical field of a standard lymph node dissection.[91-93] For these reasons choline-PET/CT for detecting metastases to lymph nodes has been commonly used in Europe since 2010 (Figure 9).[73]

For staging of bone metastases choline PET/CT has consistently shown more accuracy than bone scan in its ability to detect both bone and bone marrow metastases (Figure 10).[94] It also has higher image resolution.[95-97] In patients with intermediate to high-risk prostate cancer it was found that choline-PET/CT was more sensitive and specific at detecting bone marrow metastases than bone scan or CT alone. For bone metastases they reported a 100% sensitivity and a 90% specificity with choline-PET compared to bone scan.[95] One study showed an advantage of choline-PET/CT over MRI or MRI DWI for detecting bone metastases in 47 high risk patients.[88] It should be noted that many of the studies were performed on intermediate to high risk patients. In the

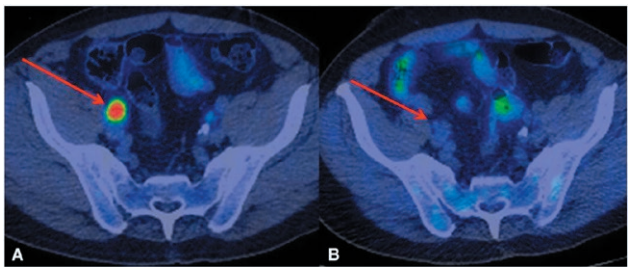

Figure 9. A shows a right external iliac lymph node with a large uptake of ^{11}C-choline. **B** shows the same area after 4 months of successful treatment.[24]

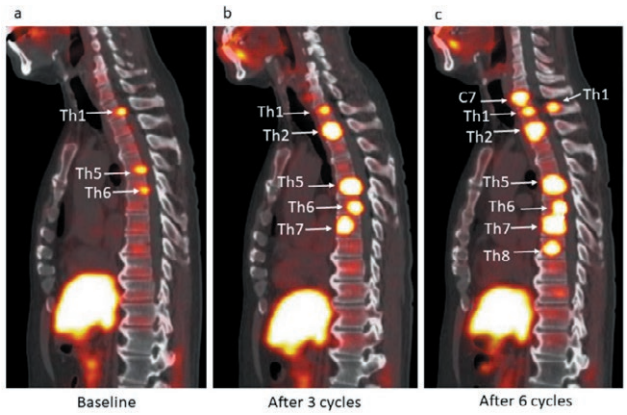

Figure 10. a to **c** clearly shows the progression of bone metastases during multiple cycles of treatment. The large bright spot in the lowest part of the figure is the normal liver which concentrates the ^{11}C-choline that is injected. Th is thoracic vertebrae, C is cervical vertebrae.[94]

higher risk patients, the sensitivity of choline-PET/CT increases dramatically.

Restaging after Relapse (Treatment Failure)

Many men treated for prostate cancer relapse and need to be restaged. In the vast majority of cases the relapse is found by an increase in the Prostate Specific Antigen (PSA). This is also called biochemical recurrence (BCR) in prostate cancer. PSA is an enzyme found predominantly in the cytosol of prostate cells.[24] For most men without prostate cancer the normal serum level is about 0.7 ng/ml and in prostate cancer it can increase dramatically to 100 or 1000 ng/ml but in most cases levels above 6 to 10 are worrisome. Most men treated for high-risk prostate cancer have the prostate and pelvic lymph nodes removed at the time of initial diagnosis. In these men the PSA level goes below 0.2 ng/ml. An increase of the PSA on two measurements taken 3 months apart indicates recurrence. For men treated only with radiation therapy without removal of the prostate an increase of 2 ng/ml from the lowest measurement during treatment indicates recurrence, sometimes called biochemical failure.[73]

As in the initial staging, mpMRI proved to be superior to choline-PET scanning for locating a recurrence in the prostate or in the prostate area of men who had undergone prostatectomy.[98, 99] Where choline PET/CT stood out was its ability in restaging after treatment failure to detect lymph node and bone metastases.[83] Choline PET/CT showed an overall sensitivity for recurrence in the lymph nodes, bone, and other sites in 86 to 89% of patients and its use is recommended by the European Association of Urology.[90, 100-102] This far exceeded the detection rate of FDG-PET and mpMRI. For detection of all lymph nodes compared to the surgical dissection of the lymph nodes after recurrence, the sensitivity was about 60%.[103-107] These sensitivities make it far superior to FDG-PET[81, 105] and mpMRI[99] for restaging of local and more distant lymph node metastases.

Of note, Choline-PET/CT findings at restaging have allowed for site directed radiation therapy to target the area and to calculate the radiation dose. This directed "salvage radiation therapy" by choline-PET/CT has led to improved disease free survival.[108-110] One study showed that a combination of salvage lymph node dissection and radiation therapy in patients led to a 70% five year disease free survival in patients staged with choline-PET/CT.[111]

In addition to its usefulness in detecting relapse into the lymph nodes choline-PET/CT was able to detect prostate cancer in 15% of patients with negative bone scans and is equivalent to mpMRI for detecting bone metastases.[101, 99] Another advantage of choline-PET/CT is its ability to detect the more aggressive osteolytic metastases.[112] This allows corrective treatment to be started to prevent fractures of those bones. For these reasons, choline-PET/CT is often the preferred imaging technique in relapsed prostate cancer treatment failures[24, 73, 83] and is commonly recommended in treatment guidelines.[113, 90]

Historical Guidelines for use of Choline-PET for Prostate Cancer

The European Association of Urology (EAU) Guidelines on Prostate Cancer[90] first mentions the use of choline-PET/CT in the 2010 guidelines for locating metastases to bone during initial staging, but states that the use in relapse is unclear. By 2015, the guidelines did not recommend choline-PET/CT for initial staging. But for staging in relapse, choline-PET/CT was useful for detecting lymph node and bone metastases if the serum PSA level was greater than 1 to 2 ng/ml and was more sensitive than bone scan. By 2018, the EAU guidelines gave a ***strong*** recommendation for the use of choline-PET/CT or PSMA-PET/CT following BCR after radiotherapy to stage local lymph node metastases or distant metastases to bone or other tissue. The 2021 guidelines discuss that choline-PET/CT can be used for detecting bone (but not lymph node) metastases at initial staging and will simultaneously detect bone and other more distant metastases, but it is not a strong recommendation. For cases involving relapse after radiotherapy the 2021 EAU does give a strong recommendation for choline-PET/CT or

PSMA-PET/CT for patients being considered for curative lymph node salvage treatment and can change management in up to 48% of patients.

It is noticeable that the formal recommendations are more conservative than what is reported above as actual common use of choline-PET/CT in initial staging and restaging. However, the recommendations are consistent with publications highlighting that it is more sensitive in cases of relapse than at the initial staging. One reason for this may be that the biochemical studies on cancer cells show that the levels of PC increase as the cells become more malignant. With relapse it is the more malignant and aggressive cells that predominate.

PSMA PET scan for prostate cancer

PSMA is a folate hydrolase glycoprotein[24] that, despite its name, is found in more tissue than just prostate. Despite the similarity of the name this is a different protein enzyme than Prostate Specific Antigen (PSA) which is mostly in the cytosol of prostate cells. In prostate cancer PSMA is overexpressed by 100 to 1000-fold. A newer PSMA PET agent Gallium-68 PSMA-11 was recently approved by the FDA in Dec 2020[114, 115] and has been used and studied in Europe and Australia since 2015.[116, 117] Many recent papers claim it is more sensitive and specific than choline-PET at lower levels of PSA and future head to head comparisons are being planned. There have been other PSMA-PET tracers developed. Since PSMA is an enzyme, they have in common that they target the substrate recognition site on PSMA. To date it is Gallium-68 PSMA that has been the most studied. It should be noted that "PSMA PET tracer" refers to the whole family of PSMA tracers and not to any one in particular.

Correlation with Prostate Surface Antigen (PSA) level for Choline and Gallium 68 (Ga-68)

It has been noticed that there is a strong correlation between the sensitivity of a PET imaging agent to detect prostate cancer in patients, and the serum level of PSA. This is because the higher the serum PSA the more advanced the cancer. It has become the norm to divide the sensitivity of PET imaging agents into 3 categories. The sensitivities below a PSA of 1 ng/ml, those sensitivities for PSA levels between 1.0 to 2.0 ng/ml and the sensitivities for a PSA level above 2.0 ng/ml.[24] A recent review[24] in patients with a relapse showed Ga-68 PSMA to be more sensitive at all levels. The authors cautioned that this was pooled data from multiple studies, and they were not standardized. However prospective head-to-head studies of choline vs Ga-68 PET/CT scanning is underway.

Multiple studies published in 2020 and 2021[116, 118, 117] also show that Ga-68-PET/CT is more sensitive than choline PET/CT and is replacing choline PET/CT in many centers. However, the experience gained with choline PET/CT over the past 20 years cleared the way and is influencing and guiding the applications of Ga-68 PET/CT. Basically, they are the same applications such as staging and guiding of therapy but with a more sensitive agent. It remains to be seen if choline-PET/CT will still have applications that Ga-68 cannot be used for in prostate cancer and other cancers.

CHOLINE KINASE AS A TARGET OF CHEMOTHERAPY

The earliest PL enzyme target for chemotherapy and the one most studied has been CK.[119] However other enzymes in the pathway have also been proposed as targets.[120] The development of CK inhibitors for possible cancer treatment has been closely connected to the biochemical studies on this enzyme and its importance in two different functions: 1) cancer transformation and 2) the catalyzing of choline and ATP to produce PC. By 1998, it had become clear that there were two forms of CK – an alpha and a beta form and their amino acid sequence had been determined.[121] Subsequent studies showed CK alpha to be the more important isoform in cancer.[122] To date the most potent CK alpha inhibitors developed have been MN58b and RSM-932A which is also called TCD-717.[27, 119]

The first paper published on interfering with the PL pathways by CK inhibition was in 1974.[123] The compound used was purinyl-6-histamine and had been observed to be cytotoxic to tumor cells *in vitro* with little to no effect on normal cells *in vitro* or to have any effect on DNA or proteins. The study made "preliminary observations" about purinyl-6-histamine's effects as a CK inhibitor and the morphological changes observed in the membrane of cancer cells being more pronounced than those of normal cells, but there were no follow-up publications.

There were two more papers published in 1983[124] and 1985[125] studying the effects of Hemicholinium-3 (HC-3) on Krebs II ascites carcinoma cells. They found that HC-3 inhibited both the choline transport mechanism across the cell membrane and also inhibited CK intracellularly. They also found that the synthesis of PtdCho was diminished in Krebs II ascites carcinoma cells by HC-3 but not in normal liver cells.

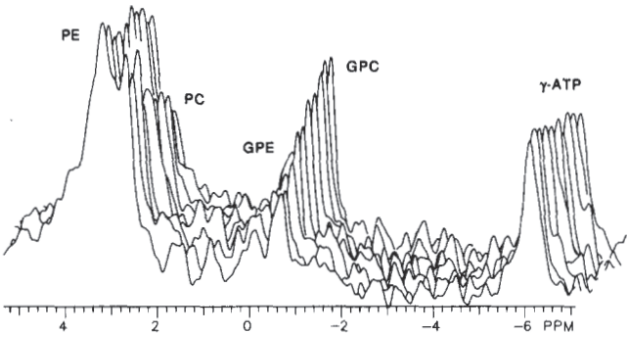

Figure 11. Effect of HC-3 in the perfusate. Quantitative 31P NMR spectra are depicted of cells grown in IMEM with 15 mM choline and 10 mM ethanolamine, harvested at log phase, and then perfused with Buffer A, 11 mM glucose, plus 100 mM HC-3. Each spectrum represents a 1-h accumulation.[13]

In 1987 the ^{31}P NMR spectra of MDA-MB-231 cancer cells were monitored while being observed in intact cells being perfused in the NMR spectrometer by a buffer solution without any choline. The introduction of HC-3 into the perfusate caused a reduction of the PC peak by over 50% in 8 hours (Figure 11).[13] This would indicate that the reduction in the PC peak observed in this experiment was due to inhibition of CK and not only to inhibition of choline transporters. HC-3 would become the template that most future CK inhibitors would be based on.[27, 119]

As discussed in the section on "Applications of MRS," subsequent studies done in the 1990's confirmed that most cancer cells studied had high levels of CK and PC. A review article by Podo referred to 1983 to 1993 as the "pioneering decade"[19]. MRS studies on cells grown *in vitro* led to the hypotheses that the increased PE and PC levels in cancer cells were involved in cell membrane synthesis, and cell growth in cancer cells,[13, 126, 127, 15] and that "specific oncogenes resulted in the increased production of choline and ethanolamine kinase."[16] These observations triggered further studies and confirmation of the hypotheses involving the PL pathways and the enzymes and oncogenes involved.

Most of the studies have focused on CK.[17, 120] Further studies showed that the CK alpha gene also functions as an oncogene involved in tumor initiation and progression.[120, 128, 129] Of the alpha and beta forms only CK alpha has been found linked to tumor transformation. Increased expression of CK alpha 1 is oncogenic to cells, but overexpression of CK beta is not. Increased production of CK alpha 1 mRNA is found in breast and lung cancer cell lines, but there is no change in CK beta mRNA levels.[122]

From 1987 to 1995 multiple papers were published showing that the ras oncogene causes an activation of the CK enzyme[130, 34, 131-136] causing an increase in PC. Data from one of the papers[34] indicated that PC may function as a second messenger in cells involved in cell growth. At that time HC-3, which was first reported in 1974[137] was the most potent inhibitor of CK and served as the template for the development of numerous CK inhibitors that fall into two categories: 1) bis-pyridiniums and 2) bis-quinoliniums.[27, 119] HC-3 itself had a paralyzing respiratory effect at therapeutic levels for treating cancer,[138] so CK inhibitors were developed that were both more effective with no or reduced side effects *in vivo*.[27, 119]

In 1997, numerous bis-pyridiniums were produced in the lab of Juan Carlos Lacal[131] and the compound named MN58b proved to be the most effective. NIH3T3 cell lines that had been transformed by ras, src, and mos oncogenes were profoundly inhibited in their growth by the new bis-pyridiniums CK inhibitors by a factor of 600 to 1000 and were effective in the low micromolar range.[139] The ras, src, and mos transformed cells had elevated levels of CK activity and the degree of inhibition correlated with reduced production of PC. MN58b was later shown to significantly inhibit the growth of xenograft tumors.[140, 139, 141] Later studies showed that MN58b was 20 fold more effective at inhibiting the CK alpha enzyme compared to the beta form of the enzyme.[27, 122]

The next set of new CK inhibitors studied were in the bis-quinolinium class. In 2005 Lacal's laboratory studied forty more compounds and compound 40 was the most potent in the bis-quinolinium class.[142] It was subsequently labeled as RSM-932A and is also called TCD-717. TCD-717 completed a Phase 1 study in solid tumors in 28 patients between Jan 2011 and February 2014.[143] TCD-717 was selected for the Phase 1 trial as it has no detectable toxicity in mice at levels that cause 77 percent tumor growth inhibition *in vivo*. In addition, it caused reversible cell cycle arrest in nontumor cells but cell death via apoptosis in cancer cells.[144] The study was sponsored by Translational Cancer Drugs Pharma which is located in Spain, but the studies were conducted at Johns Hopkins University and the Barbara Ann Karmanos Cancer Institute in Detroit, Michigan. To date results of the Phase 1 trial have not been published, but in 2021[119] Lacal referring to the Phase 1 trial stated that "the toxicology studies have already been addressed" and indicated that RSM932A/TCD717 has "paved the way for future development".

RSM932A/TCD717 has a unique mechanism of action and was found to ***not*** bind to the pockets on CK alpha where choline and phosphate are catalyzed like

other CK alpha inhibitors bind, but to bind to the surface of the enzyme.[145] This caused both a severe reduction in both PC and in the levels of CK alpha. One hypothesis is that RSM932A/TCD717 causes a drastic reduction of the level of CK alpha protein by causing a conformational change that makes it susceptible to proteases.[119] In some tumors inhibition of CK alpha with no reduction in CK alpha levels within the cell is insufficient to cause cell death.[146, 147] However, in glioblastoma cells inhibition of CK alpha by pure enzyme function inhibitors such as V11-0711 that has no effect on the level of the enzyme is sufficient to lead to tumor cell death.[119] The mechanism of cell death in tumors by CK inhibitors may vary depending on the cell type.

A 2021 review article titled "Recent Advances in the design of small molecule CK alpha inhibitors and the molecular basis of their inhibition" shows that this remains an active area of research.[28] In addition to small molecule inhibitors, siRNAs (silencing RNAs) have also been developed against CK alpha and phospholipase D and are under active study and produce reduced cell proliferation in xenographic tumors but have not yet reached Phase 1 patient studies.[120]

DEVELOPMENT OF CLINICAL APPLICATIONS OF MRS/MRSI/MRI

Introduction: Magnetic Resonance Spectroscopy (MRS) of tissue metabolites in a freshly amputated frog leg was first reported in 1974 by D.I Hoult et. al. in George Radda's research group at Oxford where they observed phosphate metabolites by ^{31}P MRS.[148] In that first report they labeled the observed peaks as sugar phosphates, PL, Pi, creatine phosphate, and the gamma, alpha, and beta peaks of ATP. This was one year after the first paper on the feasibility of Magnetic Resonance Imaging (MRI) was published by Paul Lauterbur.[149] Since the late 1980s MRI and MRS have been closely linked, with localized MRS being recorded after an MRI is obtained.

In 1980 the earliest *in vivo* human MRS was reported by J.D. Cresshull et. al. in Radda's lab observing the ^{31}P spectra from a human arm and the effects on PCr (phosphocreatine) and Pi before, during, and after the removal of a tourniquet.[150] The first *in vivo* spectrum of a human tumor was done by ^{31}P MRS in 1983 by Griffiths et al.[151] of a rhabdomyosarcoma and showed prominent peaks in the PME region and the PDE region not seen in normal muscle. The PME area is now known to be PE and PC but was assumed to be sugar phosphates at that time.

In 1985 *in vivo* ^{31}P MR spectra of neuroblastomas in two children with metastases to liver and muscle showed a high concentration of PMEs in the tumor compared to the ^{31}P NMR spectra of the normal liver and muscle tissue *in vivo* in the same children, which showed much smaller PME peaks. The large PME peak returned to normal size if the neuroblastoma was successfully treated or if it spontaneously regressed (a common feature for neuroblastoma in infancy). This initial observation of 1) a high PME peak that 2) diminishes with resolution of the tumor has been one of the main uses of MRS in cancer ever since. The PME peak in neuroblastoma was assigned to PE at 10 mM concentration, with a smaller contribution from PC and 2,3-DPG (2,3- Disphosphoglycerate).[152] They also reported a small PDE peak which in high resolution ^{31}P MRS of biopsy material was identified as GPE and GPC.

As was discussed earlier in the section on Application of MRS, extracts and cell studies were also done concurrently with the early *in vivo* ^{31}P MR studies. At that time there were conflicting reports of the origins of the PME peak in cells and *in vivo* from tumors. Many early ^{31}P MR studies assigned the PME peak to sugar phosphates. Others assigned the PME peaks to PC and PE using acid extracts of cancer cells,[19] but the enzymes creating these peaks were not determined. In 1987 the first ^{31}P MRS studies of cancer cells in real time *in vitro* studied with enzyme substrates and inhibitors (Figure 7) confirmed the PME peaks were predominantly PE and PC; and they were produced by CK and ethanolamine kinase in the Kennedy pathways, and the PDE peaks were mostly GPC and GPE.[13]

By 1989 *in vivo* ^{1}H spectra of human brain and brain tumors were being published which showed multiple metabolites in the ^{1}H spectra, including a large peak that was a combined peak of choline, PC, and GPC called the total choline peak or tCho peak.[153, 23] Biochemical studies established that the dominant peak in the tCho peak is PC with a contribution from GPC and a smaller contribution from free choline.[17] Since that time most *in vivo* spectra of cancer in humans have been ^{1}H spectra since it has greater sensitivity and can be obtained from smaller volumes than ^{31}P spectra.[18] Because MRS can measure some metabolites localized *in vivo* it has always held out the promise that it could be useful for diagnosis and monitoring of treatment.

It is the unique radiofrequency of the two hydrogen atoms in water that provide the images obtained by clinical MRI machines. The hydrogens in fat also contribute somewhat to the images. Water is 55.5 Molar which means the two hydrogen atoms in water are at 111 Molar. Due to this high concentration the ^{1}H radi-

ofrequency of water observed from the human body produces a very strong peak with an extremely high signal to noise ratio. Because water does not make up 100% of the volume of human tissue the signal is correspondingly decreased. By contrast, the concentration of other metabolites seen by ^{31}P or ^{1}H MRS such as PC, PE, GPC, GPE are in the range of 1 to 10 millimolar or .001 Molar to .01 Molar. This is a concentration difference of approximately 10,000 to 100,000 fold and makes obtaining spectra from patients reliably, quickly, reproducibly, easily, and with a high signal to noise very difficult and has been the major barrier to the widespread use of MRS in medicine, despite major attempts over the past 30 years.[154, 155] As of today, common use of single voxel MRS or multivoxel MRSI occurs in major research hospitals, but not in community hospitals where the vast majority of MRI machines are located.

The two main MR nuclei used *in vivo* have been ^{31}P and ^{1}H spectra. Of the two, ^{1}H has been used more often since ^{1}H has 16 times intrinsically more signal intensity than ^{31}P.[148] Also PC and GPC have 9 hydrogens in the trimethyl part of choline that give off the identical radiofrequency signal (see Figure 2) that also increases the signal to noise ratio. The main disadvantage of ^{1}H spectra is that choline, PC, and GPC have their radiofrequency signal so close together that *in vivo* it is just one peak called the tCho peak.

Although *in vivo* spectra have been used in areas other than cancer, these studies mostly involve peaks in the spectra not related to PL metabolism.[156] Whereas its use in aiding in the diagnosis of cancer and monitoring of therapy has relied predominantly on the PC and GPC peaks; and to a lesser extent, the PE and GPE peaks when ^{31}P NMR is used. The three areas of cancer where it has been used the most is in brain, breast, and prostate cancer. As of 2021, 354 clinical trials were found under the search "cancer and magnetic resonance spectroscopy" at clinicaltrials.gov. About 80% of NIH clinical trials have been in brain, prostate, and breast cancer, in that order.[157]

MAGNETIC RESONANCE SPECTROSCOPY AND SPECTROSCOPIC IMAGING IN BRAIN TUMORS

Localized ^{1}H MRS of the human brain was first reported in 1985[158] and multiple papers on high resolution ^{1}H MRS of the human brain soon followed.[159, 160] As of today multiple resonances can be observed by ^{1}H MRS of the brain and brain tumors which include tCho, NAA (N-acetyl aspartate), total Creatine (tCr), Glutamate/glutamine (often abbreviated Glx), Lactate (Lac), Alanine (Ala), Lipids, Myo-inositol, and a broad macromolecule peak.[161, 26] Usually the tCho peak is just called "the choline peak" and the tCr peak is just referred to as "creatine". 2-Hydroxyglutarate was first seen in 2012.[162] By 1989 Frahm et. al reported on 8 primary brain tumors and one metastatic breast cancer tumor to the brain.[153, 160] They found the spectra were remarkably different from normal brain tissue by having a high tCho peak and a low NAA peak. But histologically similar tumors gave similar spectra to each other. Similar results were reported on spectra obtained at 4 Tesla in 1989.[163] The tCho peak has been found to be predominantly PC[164, 26] and NAA is a marker of normal neuronal tissue.[165, 26] These papers looked at gliomas, meningiomas, one neurilemmoma, one arachnoid cyst, and one metastasis due to breast cancer. They concluded ^{1}H MRS may become an important tool for differentiation of tumors as well as for planning and following therapy. They also concluded that the ^{1}H MRS method was better than ^{31}P MRS since spectra could be obtained on smaller voxels which avoided sampling both the tumor and the surrounding normal tissue.[163]

These early studies were single voxel studies. However, in 1982 Truman Brown published on NMR chemical shift imaging (CSI)[166, 167] where spectra are obtained from multiple voxels adjacent to each other in a square grid of n by n voxels; and then a gray or color scaled image of the intensity of a metabolite such as choline can be made from the individual spectra in each voxel. This can be extended to a cube that is n by n by n voxels. If it's a flat grid it's 2 dimensional CSI and a cube is 3 dimensional CSI. CSI is now frequently referred to as MRSI (See Figure 13 from 2021). Because the metabolites are in such low concentration compared to water these images do not give the same high resolution as standard MRI but methods for increasing their resolution have improved markedly since the late 1980s.[168]

In 1990 Luyten et al. produced MRSI of brain tumors on voxel sizes of 1.225 ml (7 by 7 by 25 mm) and produced low resolution images showing elevated tCho and decreased NAA in tumors with noticeable heterogeneity within the same tumor.[161] By 1992 ^{1}H NMR spectra on over 200 brain tumors had been reported. Some of these reports used CSI but most used single voxel spectra.[169] As of 1992 the most common observations on primary brain tumors were an elevated tCho, decreased tCr and decreased NAA (See Figure 12 from 2003).[170] tCho, tCr, and NAA are the three most prominent peaks in the ^{1}H spectra of brain and brain tumors. Metastatic cancers to the brain and gliomas frequently contained Lac whereas meningiomas, neurinomas, and lymphomas did not. Meningiomas often contained Ala.

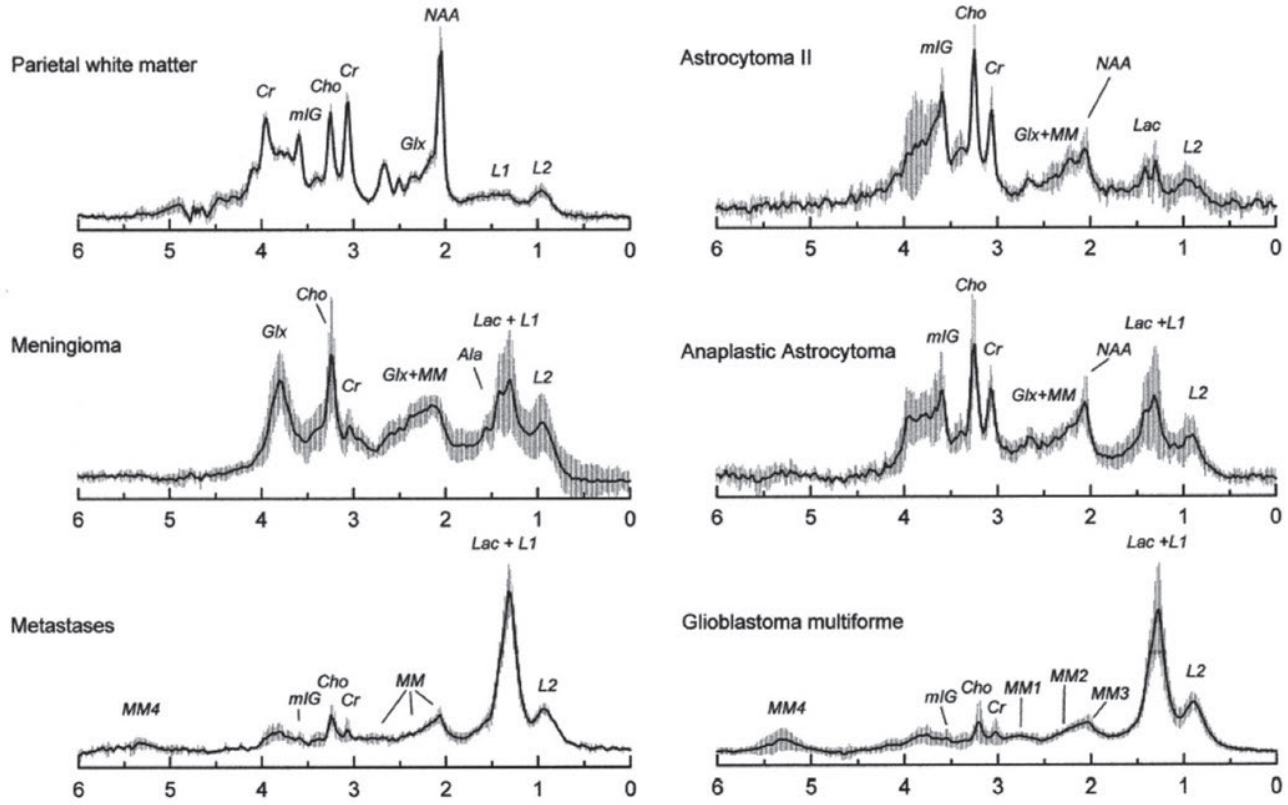

Figure 12. Spectra of normal brain tissue (parietal white matter) compared to tumors. The increased choline and decreased or absent NAA in the tumors is well demonstrated. Cr is tCr, mIG is myo-Inositol, Cho is tCho, Glx is glutamate plus glutamine, NAA is N-acetyl aspartate, L1 and L2 are lipids, Lac is lactate, MM is macromolecules, Ala is alanine which is characteristic of meningiomas.[170]

Increased PME and decreased PCr were not as commonly observed with ^{31}P MRS of brain tumors due to the large voxel sizes that would also include normal and/or necrotic tissue and would dilute the tumor signal.[169] By the mid to late 1990s most brain MRS was ^{1}H MRS. Increased tCho and decreased NAA and decreased tCr are still the most reliable change in the spectra from normal to malignant brain tissue seen in ^{1}H MRS or MRSI of brain tumors.[26]

In 1996 a pilot study using ^{1}H MRS was done to see if it could distinguish between recurrent or residual brain tumor vs delayed cerebral necrosis in children following radiation therapy since this could not be done by standard imaging techniques.[171] 12 children were studied by ^{1}H MRS and the results were confirmed by biopsy. Markedly decreased tCho, tCr, and NAA were expected to indicate necrosis and easily visible tCho and tCr was expected to identify residual or recurrent tumor tissue. Biopsies were done after the spectra and MRS identified 5 out of 7 patients with tumor and 4 out of 5 patients with necrosis. The conclusion was ^{1}H MRS showed promise for differentiating necrosis from tumor. As of 2021 this is one of the common clinical uses of ^{1}H MRS.[26]

In 1996 and 1998 Preul et al used pattern recognition analysis of the six most common peaks observed in ^{1}H NMR spectra in the 1990s.[172, 173] For each profile, the metabolites were plotted by connecting peak heights with a straight line in the order with which the metabolites appear in a ^{1}H-MR spectrum from left to right: tCho, tCr, NAA, Ala, Lac, and Lipids. The most common brain tumors are gliomas, so called because they derive from glial cells. Glial cells are not neurons but non-nerve cells that support the neurons of the brain. There are 4 types of glial cells: astroctyes, oligodendroctyes, ependymal cells, and microglia. The gliomas are graded I to IV in increasing grade of malignancy. Sometimes a tumor will be referred to as a Grade II glioma or sometimes more specifically as a Grade II Astrocytoma, or Grade II Ependymoma etc; if the glial cell of origin is identified by histology. An Anaplastic Astroctyoma is a grade III Astroctyoma. Glioblastoma multiforme is a Grade IV Astrocytoma. Grade I to II are low grade. Grade III to IV are high grade.

Preul et al. reported they could correctly classify 104 out of 105 spectra which included normal brain tissue and the five most common adult brain tumors that are shown in Figure 12. Biopsies of the tumors were done after the spectra were obtained. They concluded ^{1}H MRS can "enable accurate, noninvasive diagnosis of the most prevalent types of supratentorial brain tumors".[173] However, this paper did not include the spectra of other brain disorders such as abscesses, necrosis, lymphomas, and tumefactive demyelinating lesions. It was later found that brain tumor spectra can overlap with these pathologies and this overlap reduces the accuracy of ^{1}H MRS of brain tumors to 60 to 80% and has been the primary reason MRS is not used more frequently in the diagnosis of brain tumors.[26]

By the end of the 1990s into the early 2000s pattern recognition techniques were being used by several groups to diagnose different types of tumors by ^{1}H MRS or MRSI.[174-176] In Europe a multicenter project called "INTERPRET" was set up to give computer-based decision support to radiologists in diagnosing and grading brain tumors. Spectra were collected from 334 patients from 2000 to 2002 and used automated pattern recognition.[177, 178] Another project called eTUMOUR from 2004 to 2009 expanded the INTERPRET approach.[177] But these techniques have not been easy to transfer to general radiology clinical practice due to difficulty of obtaining spectra, the overlap in appearance of spectra of different tumors, and heterogeneity within the same tumor.[179]

CURRENT ESTABLISHED CLINICAL AREAS:

The studies done from 1989 to 2010 established the areas that are most useful now for ^{1}H MRS/MRSI in brain tumors. Further studies from 2010 to 2021 solidified these areas. Those areas are: **1) Diagnosis**, particularly of masses on the MRI that can mimic primary brain tumors in appearance, **2) Grading** of tumors which also relates to prognosis, **3) Post treatment evaluation**, especially for differentiating growth of the tumor from radiation effects, and **4) Treatment planning** for biopsy, surgical resection, and radiation therapy.[26, 180] The first 3 are used clinically and the fourth area is currently an active area of research.[26] The clinically useful areas are covered by some insurers.[180, 181] By 2020 it was established that **elevated tCho and reduced tCr and NAA** in primary brain tumors are the most important observations and the most useful ratios are tCho/NAA and tCho/tCr. The metabolites most used by 2021 are tCho, NAA, tCr, Lac, Lipids, and Myo-inositol.[26]

1) Diagnosis

The diagnosis of brain tumors up to 2010 has been previously discussed. From 2010 onwards more studies contributed. In the past the standard approach was first a needle biopsy of the tumor followed by surgical removal. On the MRI it may be difficult to tell a brain tumor from **metastatic disease, tumefactive demyelination, lymphoma, edema, abscess, or necrosis**. And spectra of high-grade gliomas (HGG) can overlap with other primary brain tumors and non-neoplastic disease, so MRS is not used alone but in combination with MRI and other imaging techniques This combined imaging can form a "virtual biopsy" on some, but not all, brain tumors before surgery to differentiate primary brain tumors from these other masses and the needle biopsy may not be needed.[26, 182]

One study on 69 adults from 2008 attempted to differentiate between tumors and their mimics by MRSI combined with perfusion imaging.[183] 36 of the 69 adults had brain tumors and the other 33 adults had a different diagnosis. The MRSI correctly classified 84% of the 69 lesions by using the ratios of NAA/tCho, NAA/tCr, and tCho and NAA normalized to signals from a normal area of the brain. However, when the MRSI findings were combined with perfusion imaging the specificity increased to 92% for the correct categorization. In another study from 2006 of 32 children the specificity was 78% for correct categorization, 13 of the children had tumors and 19 had a benign lesion.[164]

Both **metastases** and gliomas have elevated tCho and decreased NAA compared with adjacent normal tissue. But lipids and macromolecules can appear in the ^{1}H spectra and tend to be higher in metastases compared to gliomas.[184, 185] A study done in 2013 showed an 80% specificity using this method[26]. This illustrates that the additional peaks in the ^{1}H spectra of brain tumors add to the diagnosis rather than just relying on the increased tCho and decreased NAA levels. Gliomas often have microscopic extension into the surrounding brain tumor not seen on the MRI whereas metastases usually do not. Metastases tend to have a sharper border on the MRI. Studies published from 2004 to 2018 showed that spectra from the **edematous area** surrounding gliomas tend to have a high tCho/NAA and tCho/tCr.[184, 186, 187, 188] One study found this could discriminate a primary glioma from a metastasis with 100% sensitivity and 89% specificity.[189]

Primary central nervous system lymphomas tend to have a lower tCho/NAA ratio than primary brain tumors and lower myo-inositol.[190, 191, 192] **Tumefac-**

tive demyelinating lesions (TDL) overlap in appearance with primary brain tumors on MRI.[193] One report in 2018 found that a tCho/NAA ratio of greater than 1.72 was more consistent with HGGs than TDL.[194] Also TDL frequently has a high Lac peak usually not found in untreated brain tumors.[26] Spectra from **brain abscesses** were found to be fairly distinct. In 1995 and 2004 it was published that they tend to have decreased tCho, tCr, and NAA and often have signals from amino acids not seen in tumors.[195, 196] Similar results were found for abscesses in 2010 and 2014.[193, 197] Other observations made during 1989 to 2010 were that **necrotic areas** have low levels of most metabolites but an increased lipid signal.[179]

2) Grading of Tumors and Prognosis

Another area of importance is whether it is a high or low grade tumor. Low grade is grade I to II, high grade is III to IV. Where high grade are the more malignant tumors. Multiple studies found that the tCho level in astrocytomas correlated with the grade of the tumor. The higher the tCho level the more malignant the tumor.[164, 180, 168, 198] However, in 1993 and 2003 some high grade astrocytomas were found to have low levels of tCho perhaps due to the higher grade tumors having necrotic centers[179, 199] It was found in 2000 the spectrum could vary greatly depending on which part of the tumor was sampled.[200] ***By 2009 this led to MRSI being preferable since it accounts for the heterogeneity of tumors and necrotic areas and the voxel with the highest tCho signal can be chosen for spectral analysis and biopsy.***[201] One study in 2007 using perfusion imaging to correlate with the spectra found there was no difference in the spectra of high grade vs low grade gliomas *in areas of* ***low*** *blood perfusion*. But in the regions *with* ***high*** *blood perfusion,* the tCho, plus the glutamate plus glutamine peak; and Lac plus lipid peak, were higher in high grade vs low grade gliomas.[202] Low grade gliomas tend to have a modest choline elevation and a modest NAA reduction and usually do not have Lac peaks or lipid peaks. HGGs have more noticeable change from normal brain tissue including markedly increased tCho and decreased tCr, NAA, and myo-inositol.[203] Since decreased tCr is seen the tCho/tCr is usually higher in HGGs than in low grade gliomas. The presence of Lac and lipid peaks is more typical of Grade IV gliomas and not common in Grade III gliomas.[185] But there is still overlap in the appearance of the spectra of high vs low grade gliomas, so the use of ratios is helpful. A meta-analysis of 1228 cases in 2016 found that the tCho/tCr, tCho/NAA, and NAA/tCr ratios were the most helpful and had specificities in the 60 to 70% range.[204]

Numerous papers have been published up to this time on using MRS for prognosis (prediction of survival) independent of histologic grade.[205, 206, 207, 208] Most papers noted a high tCho/NAA ratio, and the presence of Lac and lipids were associated with a shorter survival rate in adults. A related finding was also made in pediatric brain tumors. In one paper on 76 children low tCho and low (Lac +lipid) levels compared to tCr were found to be a strong predictor of survival.[209] 2-HG (2-Hydroxyglutarate) has been used more frequently since it was first seen in 2012 and it's detection strongly indicates gliomas with isocitrate dehydrogenase mutations which tend to be low grade.[162, 26]

3) Post Treatment Evaluation

MRS has been found to be useful in differentiating between tumor progression or persistence versus radiation necrosis on the MRI following radiation treatment.[210, 211] In up to 24% of glioma patients receiving radiation therapy, radiation necrosis can develop.[179] Multiple publications from 1996 to 2017 showed increased tCho compared to normal brain tissue, or increased tCho/tCr ratios, or tCho/NAA ratios suggested recurrent tumor; whereas reduced tCho, NAA, and tCr levels implied radiation necrosis.[171, 211, 212, 213, 214, 215] In addition, radiation necrosis areas frequently showed increase lipid and Lac signals compared to tumors.[216, 217, 218] In a meta-analysis of 447 cases published in 2014 MRS has a specificity of differentiating tumor from radiation necrosis of 83% by using the tCho/tCr ratio.[219] Another meta-analysis of 203 patients published in 2017 showed MRS has performed better than other radiology techniques at differentiating radiation necrosis from tumor with a sensitivity of 91% and a specificity of 95%.[220]

4) Biopsy and Treatment Planning

^{1}H MRS or MRSI was suggested as early as 2006 and 2008 to be useful in guiding the biopsies of tumors and planning the therapy based on tumor extent and aggressiveness including targeting radiotherapy.[221, 222] This is currently an active area of research using whole brain MRSI.[26, 168, 223]

Zhong et al recently used tCho and tCho/NAA maps to guide surgical biopsies by targeting areas of high tCho or high tCho to NAA.[26, 168] (see Figure 13). Zhong et al also proposed MRSI maps such as these could be used in the future to plan radiation therapy, as have other studies.[224, 225] A future strategy would be to treat areas of highest tCho/NAA with higher dose radiation therapy. A

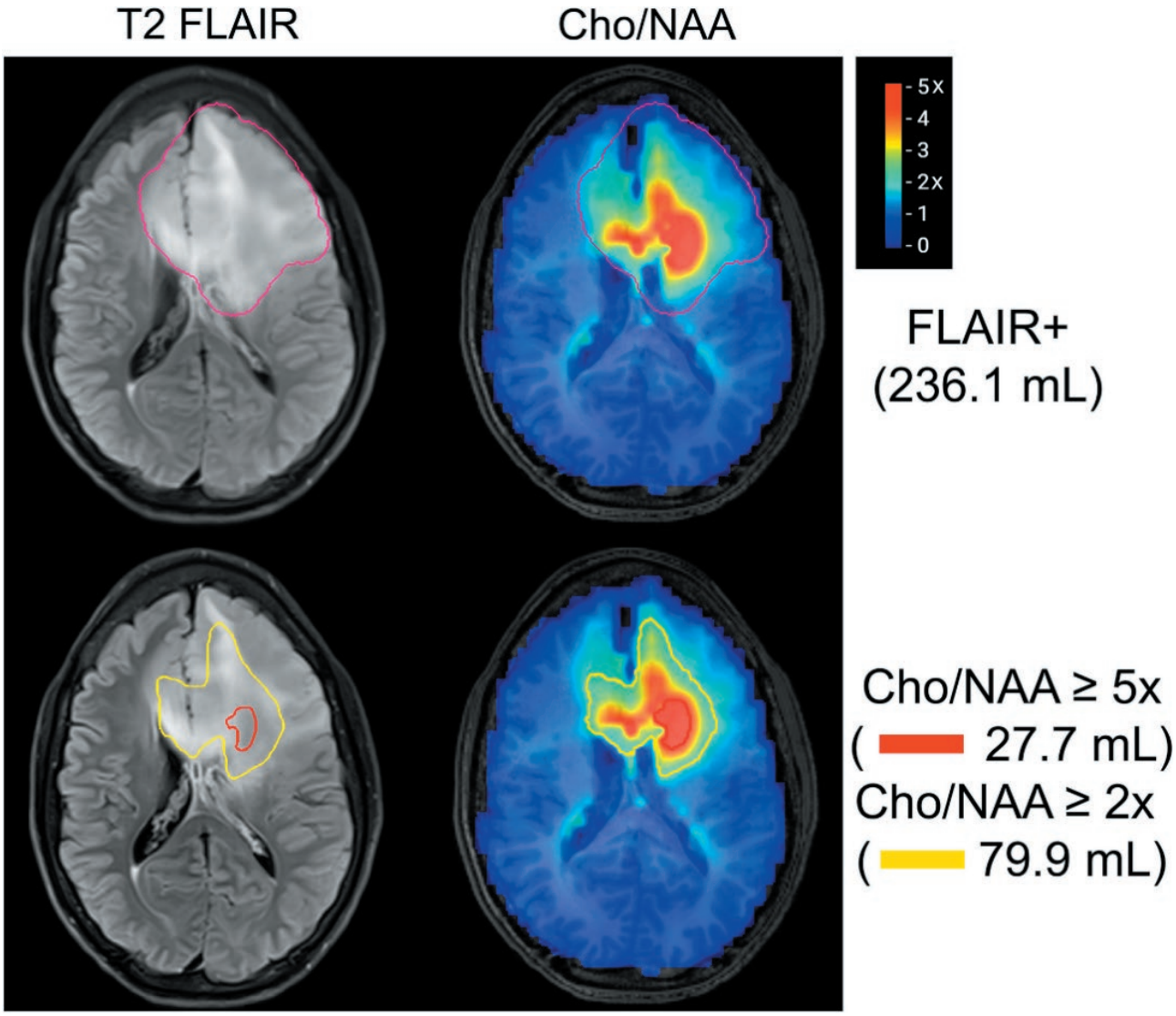

Figure 13. Upper Left Image: FLAIR image of a Grade II Astrocytoma with segmented volume of hyperintensity (pink outline) compared to Upper Right Image: T1 image overlaid with an MRSI colormap of tCho/NAA ratio. Lower Right Image: Outlined volumes show boundary for tCho/NAA of 2x (yellow) and 5x (red). The areas of highest tCho/NAA were targeted for biopsy. The upper and lower images are the same images, only the outlines are different. The tCho/NAA from normal contralateral white matter was set as equal to 1.0. Reprinted by permission from Springer Nature, Reference 168, Copyright 2021.

multisite trial was just completed and a phase II study is being planned.[226, 227]

CURRENT ESTABLISHED TECHNICAL ADVANCES IN MRS/MRSI

A major technical advance from 2010 to 2021 was a 10-fold improvement in spatial resolution. It was recognized in 2010 that one of the major limitations of MRS and MRSI was the large spatial resolution of 1 cm^3 for MRSI and 4 to 8 cm^3 for single voxel MRS was a limiting factor.[179] This greatly improved by 2021. The resolution in MRSI in Figure 13 is 0.1 ml but new developments may soon produce 2 mm by 2 mm by 3 mm resolution or 0.018 ml voxels.[168]

Currently it is mostly university research centers and a few clinical centers that are using MRS and MRSI for the clinical purposes discussed.[154, 228] The overwhelming need for transferring already existing technology at research centers for MRSI to current non-research clinical MRI machines for neuroimaging was addressed in a

2021 consensus statement written by multiple experts at leading research centers worldwide.[154] The authors pointed out that ***MRSI methods on clinical MRI machines have remained little changed in the past 20 years despite technical improvements over the past two decades that have greatly improved the quality of MRSI at research facilities producing the quality seen in Figure 13***. These improvements, primarily software updates, should bring brain MRS to the point of being an imaging modality (MRSI) and the review of the actual spectra (MRS) would be secondary. The authors pointed out they were recommending methods and uses that have already been demonstrated for neuroimaging that could be transferred to clinical practice at their current stage of development.

MRSI uses smaller voxels and can sample areas of the brain that single voxel spectroscopy cannot. The consensus group also reviewed the use of 7T MRI machines for spectroscopy although these machines are currently at research centers only and not at standard clinical radiology departments. The MRSI shown above (Figure 13) is from a 3T MRI.[168] While most clinical MRI scanners are 1.5T, commercial 3T scanners are becoming more common at both research and clinical MRI centers[229]. These higher field magnets greatly improve the speed of acquisition and resolution of MRS and MRSI. There are already many 7T MRI scanners at research centers and in 2017 clinical 7T MRI scanners were cleared for clinical use in both Europe and the USA.[230] These improvements should lead to further expansion of the reimbursement from more insurers for brain MRS and MRSI than currently exists.[180, 181]

PROSTATE AND BREAST CANCER MRS/MRSI

In addition to brain tumors, prostate and breast cancer are the other cancers that have received the most interest. But brain masses have had the most clinical success. This is due both to the nature of brain masses and technical facility. Multiple tumors can metastasize to the brain and on MRI there are multiple tumor mimics and MRSI combined with MRI is often the best method for diagnosis short of biopsy. Multiple metabolites can be seen, making MRS more useful; and both the skull and the highly sensitive nature of brain tissue make biopsy and surgery a much higher risk. Also, it is technically easier to do MRS/MRSI on the brain as it is a large organ compared to the prostate, the ability to keep the head still in a comfortable position with an MRS head coil and avoid motion artifacts due to breathing is a major advantage; and brain tumors tend to be fairly large at the time they are found.

The first ^{1}H spectra of prostate cancer using a transrectal probe was published in 1990 and showed a high citrate peak in normal prostate, and a low citrate peak in prostate cancer.[231] The first *in vivo* ^{31}P MRS of prostate cancer was published in 1991 and showed a high PME peak and PCr peak.[232] By 1996 three dimensional MRSI of the prostate with 0.24 to 0.7 ml voxels was done and multiple papers had been published showing a high tCho level and low citrate level in prostate cancer compared to normal prostate tissue.[233] The high tCho/Citrate ratio in prostate cancer is analogous to the high tCho/NAA ratio in brain tumors where tCho is a marker of malignancy and low citrate is a marker of lack of normal prostate cells. By 2012 the European Society of Urogenital Radiology (ESUR) was endorsing MRSI of prostate cancer as part of mpMRI studies of the prostate for diagnosis after relapse and for judging tumor aggressiveness and monitoring treatment response. However, they also pointed out that DWI did the same thing.[234] By 2020 mpMRI involving T1, T2, DWI, and DCE (dynamic contrast enhanced) imaging was in common use but MRSI was not.[235] Much of this had to do with technical difficulties including the use of an endorectal coil and the fact that DWI had turned out to be quicker, easier, more reproducible, and could give the same information for diagnosis, judging aggressiveness, and monitoring of therapy due to the highly cellular and unusually dense nature of prostate cancers that severely inhibits diffusion of water.[236, 155] However, further technical developments in MRS and MRSI such as avoiding an endorectal coil will likely make MRSI of the prostate useful and are still being studied.[234, 155]

By 1988 ^{1}H and ^{31}P MRS of human breast cancer *in vivo* were published. The ^{31}P spectra showed high levels of PMEs, PDEs, ATP, and Pi compared to normal tissue and these peaks reduced with successful treatment. The ^{1}H spectra showed a high water to fat ratio for the tumors of 2.2 but only 0.3 on average for normal breast tissue.[237] And by 1989 more publications appeared describing the use of ^{31}P NMR spectroscopy for monitoring breast cancer treatment *in vivo*.[238, 239] These papers noted both the increased PMEs in tumors and their decrease with treatment. By 1991 extracts of surgically removed tumors showed the broad PME region was predominantly PC and PE and the PDE region was mostly GPE and GPC as had been found in tumors in nude mice and cell studies.[16] Although many studies were done in the 1990s of breast tumors by ^{31}P MRS[240, 241] by the early 2000s most spectra were ^{1}H MRS, since it could be performed on a tumor one tenth the size and analysis of multiple ^{1}H MRS studies showed a sensitivity of 83% and a specificity of 85% at detecting breast

cancer based on the tCho peak. The specificity rose to 92% if ^{1}H MRS was combined with MRI.[242] Unlike brain and prostate there is not an additional metabolite in the breast ^{1}H MRS spectra as a marker for normal tissue similar to citrate or NAA so the determination is based almost solely on tCho. Also, there are technical problems caused by very large fat peaks in breast tissue not found in prostate and brain spectra.[156] A 2014 review pointed out that the development of MRS for breast cancer lagged behind the developments of MRS for brain and prostate but still felt it should be useful for diagnosis and monitoring of therapy.[243] But by 2019 the conclusion was still that MRS of breast tumors was "promising" and "proven to have a role in clinical care" but further work was needed in improving the technique.[244] To date MRS is not reimbursed by insurers for either prostate or breast cancer and is still considered experimental.[180]

FUTURE TRENDS IN PHOSPHOLIPID RESEARCH AND CANCER

One obvious area for future exploration is the role of the ethanolamine Kennedy pathway in cancer metabolism. Most tumors have large amounts of PE in them, often more than of PC, but this area has not been well studied biochemically or in MRS, and ethanolamine kinase-1 is found to be elevated in breast and prostate cancer cells.[245] In addition, the degradative pathways for both PtdCho and PtdEth have not been as well studied although these pathways are involved in some of the production of PC and presumably PE as well as producing second messengers involved in cell growth. And these enzymes may also be a target for therapy in addition to CK or in combination with CK inhibitors.[18, 49] And as discussed earlier, work continues on the development of CK inhibitors[119] and using MRSI of brain tumors for guiding biopsy and treatment and for prognosis.[26]

Another area that is developing is the use of ^{1}H MRS *ex vivo* on biopsy tissue or tumor tissue removed at surgery by High Resolution Magic Angle Spinning (HR-MAS). As the name implies HR-MAS involves placing tissue in a tube that is then spun at a specific angle calculated from NMR physics that results in improved signal to noise and higher resolution allowing many more metabolites to be seen than *in vivo* MRS.[246, 247] In addition, Chemical Exchange Saturation Transfer (CEST) and hyperpolarized ^{13}C are being studied.[49] Certainly, any future as yet undiscovered physical technique for in vivo MRS/MRSI that can greatly increase the signal to noise level will have a profound impact.

Choline PET is being explored for use in hepatocellular carcinomas[248] and in hyperparathyroidism.[249] Hepatocellular carcinoma is slow growing and, like prostate cancer, does not avidly take up FDG for PET scanning. Hyperparathyroidism often involves nodules of parathyroid tissue which can be difficult to localize but show up well on Choline PET scanning and the technique has been shown to be useful in a recent meta-analsis.[249]

While this is not intended to be a definitive list of all the future areas of research involving choline metabolism and choline MRS/MRSI, even a cursory review of the literature shows this to still be a very rich area for research.

CONCLUSION

The *sine qua non* of medical research is the ability to go from "bench to clinic," from basic research in the laboratory to the application to human healthcare. The subject that we have described the history of here, namely the study of PL metabolism, is an excellent example of that process. We have shown that from the earliest studies of PL metabolites in intact living cancer cells *in vitro*, it was found that the precursors and catabolites of PL can be indicators of the presence of cancer. These observations, primarily obtained by using ^{31}P MRS, were then extended and applied *in vivo* by both MRS and the vastly more sensitive methodologies of PET scanning and MRSI, to detect, diagnose and monitor treatment of patients in the clinic. This is a subject of growing clinical importance that has received the imprimatur of the medical profession and is now covered by healthcare organizations worldwide.

REFERENCES

1. Théodore Gobley, Recherches chimiques sur le jaune d'œuf [Chemical researches on egg yolk], *Journal de Pharmacie et de Chemie. 9* 81–91, **1846**.
2. Théodore Gobley, Sur la lécithine et la cérébrine [On lecithin and cerebrin], *Journal de Pharmacie et de Chimie 19* 346–53, **1874**.
3. Albert L. Lehninger, *Biochemistry.* 2nd ed., Worth, **1970**.
4. William T. Evanochko, Ted T. Sakai, Thian C Ng, N. Rama Krishna, Hyun Dju Kim, Robert B. Zeidler, Vithal K. Ghanta, R. Wallace Brockman, Lewis M. Schiffer, NMR study of in vivo RIF-1 tumors. Analysis of perchloric acid extracts and identification of proton, phosphorus-31, and carbon-13 resonances,

Biochim. et Biophys. Acta, Molec. Cell Res. 805 104-16, **1984**.
5. Britton Chance, Yuzo Nakase, Meredith Bond, John S. Jr Leigh, George McDonald, Detection of phosphorus-31 nuclear magnetic resonance signals in brain by in vivo and freeze-trapped assays, *Proc. Nat. Acad. Sci. USA 75* 4925-9, **1978**.
6. C. D'Ambrosio, B. Chance, Jr. J.S.Leigh, S. Eleff, In Vivo Phosphate Levels in Small and Large Animals, in *Noninvasive Probes of Tissue Metabolism*, ed. by J. S. Cohen, Wiley-Interscience, NY, pp. 209-23.**1982**,
7. Mildred Cohn, Thomas R. Jr. Hughes, Phosphorus magnetic resonance spectra of adenosine di- and triphosphate. I. Effect of pH, *J. Biol. Chem. 235,* 3250-3 **1960**.
8. D. L. Foxall, J. S. Cohen, NMR Studies of Perfused Cells, *J. Mag. Res. 52* 346-49, **1983**.
9. D. L. Foxall, J. S. Cohen, J. B. Mitchell, Continuous Perfusion of Mammalian Cells Embedded in Agarose Gel Threads *Exp. Cell Res. 154* 521-29, **1984**.
10. T. C. Ng, W. T Evanochko, J. D. Glickson, Faraday shield for surface-coil studies of subcutaneous tumors, *J. Mag. Res. 49* 526-9 **1982**.
11. R. C. Lyon, P. F. Daly, J. S. Cohen, Effects of Drugs on the Metabolism of Human Cancer Cells in Vitro and Implanted in Mice Monitored by Magnetic Resonance Spectroscopy, in *NMR Spectroscopy and Drug Development,*, ed. by J. W. Jaroszewski, J. Schaumberg, M. Kofod, Benzon Fndtn. Symp,, Copenhagen, Vol. 26, pp. 508-29.**1988**,
12. R. C. Lyon, R. G. Tschudin, J. S. Cohen, A Versatile Multinuclear Probe Designed for In Vivo NMR Spectroscopy: Applications to Subcutaneous Human Tumors in Mice, *Mag. Res. Med. 6* 1-14, **1988**.
13. P. F. Daly, R. C. Lyon, P. J. Faustino, J. S. Cohen, Phospholipid metabolism in cancer cells monitored by 31P NMR spectroscopy, *J. Biol. Chem. 262* 14875-78, **1987**.
14. R. C. Lyon, J. S. Cohen, P. J. Faustino, F. Megnin, C. E. Myers, Glucose Metabolism in Drug-Sensitive and Drug-Resistant Human Breast Cancer Cells Monitored by Magnetic Resonance Spectroscopy, *Cancer Res. 48* 870-77, **1988**.
15. J. Ruiz-Cabello, J.S. Cohen, Phospholipid metabolism as indicators of cancer cell function, *NMR Biomed. 5* 226-33,, **1992**.
16. P. Daly, J. S. Cohen, Magnetic Resonance Spectroscopy of Tumors and Potential in vivo Clinical Applications: a Review, *Cancer Res. 49* 770-79, **1989**.
17. Kristine Glunde, Zaver M. Bhujwalla, Sabrina M. Ronen, Choline metabolism in malignant transformation, *Nature Reviews Cancer 11* 835–48, **2011**.
18. Kristine Glunde, Marie-France Penet, Lu Jiang, Michael A Jacobs, Zaver M Bhujwalla, Choline metabolism-based molecular diagnosis of cancer: an update, *Expert Rev Mol Diagn. 15* 735–47, **2015**.
19. Franca Podo, Tumour phospholipid metabolism, *NMR in Biomedicine 12* 413-39, **1999**.
20. Gengshu Wu, Dennis E. Vance, Choline kinase and its function, *Biochem. and Cell Biol. 88* 559-64, **2010**.
21. Vladimir Sklenar, Ad Bax, A new water suppression technique for generating pure-phase spectra with equal excitation over a wide bandwidth, *J. Mag Res. 75* 378-83, **1987**.
22. P A Bottomley, Spatial localization in NMR spectroscopy in vivo, *Ann. NY Acad. Sci. 508* 333-48, **1987**.
23. P. C. M. van Zijl, C. T. W. Moonen, J. Gillen, P. F. Daly, J. F. Frank, T. F. DeLaney, O. Kaplan, J. S. Cohen, Proton magnetic resonance spectroscopy of small regions (1 mL) localized inside human tumors: a clinical feasibility study, *NMR Biomed. 3* 227-32, **1990**.
24. Jaden D. Evans, Krishan R.Jethwa, Piet Ost, Scott Williams, Eugene D.Kwon, Val J. Lowe, Brian J. Davis, Prostate cancer–specific PET radiotracers: A review on the clinical utility in recurrent disease, *Practical Radiation Oncology 8* 28-39, **2018**.
25. Michael J. Phelps, Metabolic Imaging and Positron Computed Tomography, in *Noninvasive Probes of Tissue Metabolism*, ed. by J. S. Cohen, Wiley-Interscience, NY, pp. 225-64.**1982**,
26. BD. Weinberg, M. Kuruva, H. Shim, ME. Mullins, Clinical Applications of Magnetic Resonance Spectroscopy in Brain Tumors: From Diagnosis to Treatment, *Radiol. Clin. North Am. 59* 349-62, **2021**
27. Sean P. Arlauckas, Anatoliy V. Popov, E. James Delikatny, Choline kinase alpha-Putting the ChoK-hold on tumor metabolism, *Progress in Lipid Research 63* 28-40, **2016**.
28. Belén Rubio-Ruiz, Lucía Serrán-Aguilera, Ramón Hurtado-Guerrero, Ana Conejo-García, Recent advances in the design of choline kinase α inhibitors and the molecular basis of their inhibition, *Medicinal Res. Rev. 41* 902-27, **2021**.
29. Eugene Kennedy, The function of cytidine coenzymes in the biosynthesis of phospholipides, *J. Biol. Chem. 222* 193 – 214, **1956**.
30. E. Iorio, D. Mezzanzanica, P. Alberti, F. Spadaro, C. Ramoni, S. D'Ascenzo, D. Millimaggi, A. Pavan, V. Dolo, S. Canevari, F. Podo, Alterations of choline phospholipid metabolism in ovarian tumor progression, *Cancer Research 65* 9369–76, **2005**.

31. Federica Gibellini, Terry K.Smith, The Kennedy pathway-De novo synthesis of phosphatidylethanolamine and phosphatidylcholine, *IUBMB Life 62* 414-28, **2010**.
32. Steven L. Pelech, Dennis E. Vance, Regulation of phosphatidylcholine biosynthesis, *Biochim. Biophys. Acta 779* 217-51, **1984**.
33. H. Cai, P. Erhardt, J. Troppmair, M. T. Diaz-Meco, G. Sithanandam, U. R. Rapp, J. Moscat, G. M. Cooper, Hydrolysis of phosphatidylcholine couples Ras to activation of Raf protein kinase during mitogenic signal transduction, *Mol. Cell. Biol. 13* 7645-51 **1993**.
34. A. Cuadrado, A. Carnero, F. Dolfi, B. Jimenez, J. C. Lacal, Phosphorylcholine: a novel second messenger essential for mitogenic activity of growth factors, *Oncogene 8* 2959-68, **1993**.
35. J. H. Exton, Phosphatidylcholine breakdown and signal transduction, *Biochim. Biophys. Acta. 1212* 26-42, **1994**.
36. Steven L. Pelech, Dennis E. Vance, Signal transduction via phosphatidylcholine cycles, *Trends Biochem. Sci. 14* 28-30,, **1989**.
37. M. Malumbres, M. Barbacid, RAS oncogenes: the first 30 years, *Nature Reviews, Cancer 3* 459–65 **2003**.
38. Eric O. Aboagye, Zaver M. Bhujwalla, Malignant Transformation Alters Membrane Choline Phospholipid Metabolism of Human Mammary Epithelial Cells, *Cancer Res. 59* 80-84, **1999**.
39. Raj K. Gupta, Jeffrey L. Benovic, Zelda B. Rose, The determination of the free magnesium level in the human red blood cell by phosphorus-31 NMR, *J. Biol. Chem. 253* 6172-6 **1978**.
40. L. Jacobsen, J. S. Cohen, Improved Technique for the Investigation of Cell Metabolism, *Biosci. Rep. 1* 141, **1981**.
41. J. S. Cohen, R. C. Lyon, P. F. Daly, Monitoring Intracellular Metabolism by NMR, *Methods Enzymol. 177* 435-38, **1989**.
42. R. Knop, C.-W. Chen, J. B. Mitchell, A. Russo, S. McPherson, J. S. Cohen, Metabolic Studies of Mammalian Cells by ^{31}P NMR Using a Continuous Perfusion Technique, *Biochim. Biophys. Acta. 894* 275-84, **1984**.
43. O. Kaplan, J. S. Cohen, Lymphocyte activation and phospholipid pathways: 31P magnetic resonance studies,, *J. Biol. Chem. 265* 20712-18, **1991**.
44. J. Ruiz-Cabello, J. S. Cohen, NMR and the study of pathological state in cells and tissues, *Intl. Rev. Cytology 145* 1-63, **1992**.
45. M. Sterin, J. Cohen, Y. Mardor, E. Berman, I. Ringel, Levels of Phospholipid Metabolites in Breast Cancer Cells Treated with Anti-mitotic Drugs: A 31P Magnetic Resonance Spectroscopy Study, *Cancer Res. 61* 7536-43, **2001**.
46. M. Sterin, J. Cohen, I. Ringel, Hormone sensitivity is reflected in the phospholipid profile in breast cancer cells, *Breast Cancer Res. & Treat. 87* 1-11, **2004**.
47. J. S. Cohen, R. C. Lyon, R. C. Chen, P. J. Faustino, G. Batist, M. Shoemaker, E. Rubalcaba, K. H. Cowan, Differences in phosphate metabolite levels in drug-sensitive and -resistant human breast cancer cell lines determined by 31P magnetic resonance spectroscopy,, *Cancer Res. 46* 4087-90, **1986**.
48. YL Ting, D Sherr, H Degani, Variations in energy and phospholipid metabolism in normal and cancer human mammary epithelial cells, *Anticancer Research 16* 1381-88, **1996**.
49. Kanchan Sonkar, Vinay Ayyappan, Caitlin M. Tressler, Oluwatobi Adelaja, Ruoqing Cai, Menglin Cheng, Kristine Glunde, Focus on the glycerophosphocholine pathway in choline phospholipid metabolism of cancer, *NMR in Biomedicine 32* e4112, **2019**.
50. HM Baek, JH Chen, K Nie, HJ Yu, S Bahri, RS Mehta, O Nalcioglu, MY Su, Predicting pathologic response to neoadjuvant chemotherapy in breast cancer by using MR imaging and quantitative 1H MR spectroscopy, *Radiology 251* 653-62, **2009**.
51. MA. Jacobs, PB. Barker, PA. Bottomley, Z. Bhujwalla, DA. Bluemke, Proton magnetic resonance spectroscopic imaging of human breast cancer: a preliminary study, *J Mag. Res. Imaging 19* 68-75, **2004**
52. SJ Booth, MD Pickles, LW Turnbull, In vivo magnetic resonance spectroscopy of gynaecological tumours at 3.0 Tesla, *BJOG 116* 300-3, **2009**.
53. E Ackerstaff, BR Pflug, JB Nelson, ZM Bhujwalla, Detection of increased choline compounds with proton nuclear magnetic resonance spectroscopy subsequent to malignant transformation of human prostatic epithelial cells, *Cancer Res. 61* 3599-603, **2001**.
54. J Kurhanewicz, MG Swanson, SJ Nelson, DB Vigneron, Combined magnetic resonance imaging and spectroscopic imaging approach to molecular imaging of prostate cancer, *J Mag. Res. Imaging 16* 451-63, **2002**.
55. D. Belkić, K. Belkić, In vivo magnetic resonance spectroscopy for ovarian cancer diagnostics: quantification by the fast Padé transform, *J. Mathematical Chem. 55* 349–405, **2017**.
56. A Elkhaled, L Jalbert, A Constantin, HA Yoshihara, JJ Phillips, AM Molinaro, SM Chang, SJ Nelson,

Characterization of metabolites in infiltrating gliomas using ex vivo ^{1}H high-resolution magic angle spinning spectroscopy, *NMR Biomed. 27* 578-9, **2014**
57. D Vigneron, A Bollen, M McDermott, L Wald, Day, M, S Moyher-Noworolski, R Henry, S Chang, M Berger, W Dillon, S Nelson, Three-dimensional magnetic resonance spectroscopic imaging of histologically confirmed brain tumors, *Mag. Res. Imaging 19* 89-101, **2001**.
58. S Trousil, P Lee, DJ Pinato, JK Ellis, R Dina, EO Aboagye, HC Keun, R Sharma, Alterations of choline phospholipid metabolism in endometrial cancer are caused by choline kinase alpha overexpression and a hyperactivated deacylation pathway, *Cancer Res. 74* 6867-77, **2014**.
59. P. F. Daly, Lyon, R. C., Straka, E. J., and Cohen, J. S. , 31P NMR spectroscopy of human cancer cells proliferating in a basement membrane gel, *FASEB J. 2* 2596-604, **1988**.
60. R. S. Balaban, D. G. Gadian, G. K. Radda, G. G. Wong, An NMR probe for the study of aerobic suspensions of cells and organelles, *Analytical Biochemistry 116* 450-5, **1981**.
61. A. A. De Graaf, R. M. Wittig, U. Probst, J. Strohhaecker, S. M. Schoberth, H. Sahm, Continuous-flow NMR bioreactor for in vivo studies of microbial cell suspensions with low biomass concentrations, *J. Mag. Res. 98* 654-9, **1992**.
62. Robert J. Gillies, Neil E. MacKenzie, Bruce E. Dale, Analyses of bioreactor performance by nuclear magnetic resonance spectroscopy, *Bio/Technology 7* 50-4, **1989**.
63. R. C. Lyon, P. J. Faustino, J. S. Cohen, A Perfusion Technique for 13C NMR Studies of the Metabolism of 13C-Labeled Substrates by Mammalian Cells, *Mag. Res. Med 3* 663-72,, **1986**.
64. D. L. Foxall, J. S. Cohen, R. G. Tschudin, Selective Observation of 13C Enriched Metabolites by 1H NMR, *J. Mag. Res. 51* 330-34, **1983**.
65. Y. Mardor, O. Kaplan, M. Sterin, J Ruiz Cabello, E. Ash, Y. Roth, I. Ringel, J. S. Cohen, Non-invasive real-time monitoring of intracellular cancer cell metabolism and response to lonidamine treatment using diffusion weighted proton MRS, *Cancer Res. 60* 5179-86, **2000**.
66. HM Baek, JH Chen, O Nalcioglu, MY Su, Choline as a biomarker for cell proliferation: do the results from proton MR spectroscopy show difference between HER2/neu positive and negative breast cancers?, *Int J Cancer 123* 1219, **2008**.
67. C. C. Hanstock, D. L. Rothman, T. Jue, R. G. Shulman, Volume selected proton spectroscopy in the human brain, *J. Magn. Reson. 77* 583-88, **1988**.
68. P. R. Luyten, J. A. den Hollander, C. Segebarth, D. Baleriaux, Localized 'H NMR spectroscopy and spectroscopic imaging of human brain tumors in situ, *7th Ann. Meet. Soc. Magn. Reson. Med* Abstract 252, **1988**.
69. T. Hara, N. Kosaka, N. Shinoura, T. Kondo, PET imaging of brain tumor with [methyl-11C]choline, *J. Nucl. Med. 38* 842–47, **1997**.
70. RP. Friedland, CA. Mathis, TF. Budinger, et al., Labeled choline and phosphorylcholine: body distribution and brain autoradiography: concise communication., *J. Nucl. Med. 24* 812-15, **1983**.
71. B. Scher, M. Seitz, W. Albinger, et al., Value of 11C-choline PET and PET/CT in patients with suspected prostate cancer, *Eur. J. Nucl. Med. Mol. Imaging 34* 45-53, **2007**.
72. M. Tian, H. Zhang, N. Oriuchi, T. Higuchi, K. Endo, Comparison of 11C-choline PET and FDG PET for the differential diagnosis of malignant tumors, *Eur. J. Nucl. Med. Mol. Imaging 31* 1064-72, **2004**.
73. G. Giovacchini, E. Giovannini, R. Leoncini, et al., PET and PET/CT with radiolabeled choline in prostate cancer: a critical reappraisal of 20 years of clinical studies, *Eur. J. Nucl. Med. Mol. Imaging 44* 1751, **2017**.
74. TR. DeGrado, SW. Baldwin, Wang S, et al., Synthesis and Evaluation of 18F-Labeled Choline Analogs as Oncologic PET Tracers, *J. Nucl. Med. 42* 1805 – 14, **2001**.
75. TR. DeGrado, RE. Coleman, S. Wang, SW. Baldwin, MD. Orr, CN. Robertson, et al., Synthesis and evaluation of 18F-labeled choline as an oncologic tracer for positron emission tomography: initial findings in prostate cancer, *Cancer Res. 61* 110–17, **2001**.
76. C. Brogsitter, K. Zophel, J. Kotzerke, (18)F-choline, (11)C-choline and (11)C-acetate PET/CT: comparative analysis for imaging prostate cancer patients, *Eur. J. Nucl. Med. Mol. Imaging 40 (Supp)* 18–27, **2013**.
77. P. Mapelli, E. Incerti, F. Ceci, et al., 11C- or 18F-choline PET/CT for imaging evaluation of biochemical recurrence of prostate cancer, *J. Nucl. Med. 57* 43S–8S.143, **2016**.
78. FE. von Eyben, K. Kairemo, Acquisition with (11) C-choline and (18)F-fluorocholine PET/CT for patients with biochemical recurrence of prostate cancer: a systematic review and meta-analysis, *Ann. Nucl. Med. 30* 385–92, **2016**.
79. A. Ramirez de Molina, A. Rodriguez-Gonzalez, R. Gutierrez, L. Martinez-Pineiro, Bonilla Sanchez J, F., et al., Overexpression of choline kinase is a frequent

feature in human tumor-derived cell lines and in lung, prostate, and colorectal human cancers, *Biochem Biophys Res Commun. 296* 580–83, **2002**.
80. Toshihiko Hara, 18F-Fluorocholine: A New Oncologic PET Tracer, *J. Nucl. Med. 42* 1815-17, **2001**.
81. M. Picchio, C. Messa, C. Landoni, et al., Value of [11C] choline-positron emission tomography for re-staging prostate cancer: a comparison with [18F] fluorodeoxyglucose-positron emission tomography, *J. Urol. 169* 1337–40, **2003**.
82. MD. Farwell, DA. Pryma, DA. Mankoff, PET/CT imaging in cancer: current applications and future directions, *Cancer Res. 120* 3433-45, **2014**.
83. Roger Li, Gregory C. Ravizzini, Michael A. Gorin, et al., The use of PET/CT in prostate cancer, *Prostate Cancer and Prostatic Diseases 21* 4–21, **2018**.
84. A. Roland, C. Drouet, H. Boulahdour, et al., Unusual uptakes on 18F-fluorocholine positron emission tomography/computed tomography (PET/CT): a retrospective study of 368 prostate cancer patients referred for a biochemical recurrence or an initial staging, *Quant. Imaging Med. Surg. 11* 172-82, **2021**.
85. V. Niziers, R. Boissier, D. Borchiellini, et al., "Real-world" evaluation of 18F-Choline PET/CT practices in prostate cancer patients and impact on changes in therapeutic strategy, *Urol. Oncol. 38* 2.e1-2.e9, **2020**.
86. G. Martorana, R. Schiavina, B. Corti, et al., 11C-choline positron emission tomography/computerized tomography for tumor localization of primary prostate cancer in comparison with 12-core biopsy, *J. Urol. 176* 954-60, **2006**.
87. H. Watanabe, M. Kanematsu, H. Kondo, et al., Preoperative detection of prostate cancer: a comparison with 11C-choline PET, 18F-fluorodeoxyglucose PET and MR imaging, *J. Magn. Reson. Imaging 31* 1151-6, **2010**
88. JB. Pinaquy, H. De Clermont-Galleran, G. Pasticier, et al., Comparative effectiveness of [(18) F]-fluorocholine PET-CT and pelvic MRI with diffusion-weighted imaging for staging in patients with high-risk prostate cancer, *Prostate Cancer and Prostatic Diseases 75* 323-31, **2015**.
89. L. Evangelista, F. Zattoni, A. Guttilla, et al., Choline PET or PET/CT and biochemical relapse of prostate cancer: a systematic review and meta-analysis, *Clin. Nucl. Med. 38* 305-14, **2013**.
90. N. Mottet, et al., European Association of Urology: Guidelines on Prostate Cancer, *https://uroweb.org/guideline/prostate-cancer/*, **2021**.
91. IJ. de Jong, J. Pruim, PH. Elsinga, et al., Visualization of prostate cancer with 11C-choline positron emission tomography, *Eur. Urol. 42* 18-23, **2002**.
92. R. Schiavina, V. Scattoni, P. Castellucci, et al., 11C-choline positron emission tomography/computerized tomography for preoperative lymph-node staging in intermediate-risk and high-risk prostate cancer: comparison with clinical staging nomograms, *Eur. Urol. 54* 392-401, **2008**.
93. T. Steuber, T. Schlomm, H. Heinzer, et al., [F(18)]-fluoroethylcholine combined in-line PET-CT scan for detection of lymph-node metastasis in high risk prostate cancer patients prior to radical prostatectomy: Preliminary results from a prospective histology-based study, *Eur. J. Cancer 46* 449-55, **2010**.
94. K. Kitajima, S. Yamamoto, N. Kamikonya, et al., The Potential Use of 11C-Choline Positron Emission Tomography/Computed Tomography to Monitor the Treatment Effects of Radium-223 in a Patient with Prostate Cancer, *Cureus 10* e2948, **2018**
95. L. Evangelista, M. Cimitan, F. Zattoni, et sl., Comparison between conventional imaging (abdominal-pelvic computed tomography and bone scan) and [(18)F]choline positron emission tomography/computed tomography imaging for the initial staging of patients with intermediate- to high-risk prostate cancer: A retrospective analysis, *Scand. J. Urol. 49* 345-53, **2015**.
96. H. Kjölhede, G. Ahlgren, H. Almquist, et al., Combined 18F-fluorocholine and 18F-fluoride positron emission tomography/computed tomography imaging for staging of high-risk prostate cancer, *BJU Int. 10* 1501-6, **2012**.
97. M. Picchio, EG. Spinapolice, F. Fallanca, et al., [11C]Choline PET/CT detection of bone metastases in patients with PSA progression after primary treatment for prostate cancer: comparison with bone scintigraphy, *Eur. J. Nucl. Med. Mol. Imaging 39* 13-26, **2012**.
98. F. Bertagna, M. Abuhilal, G. Bosio, et al., Role of ^{11}C-choline positron emission tomography/computed tomography in evaluating patients affected by prostate cancer with suspected relapse due to prostate-specific antigen elevation, *Jpn. J. Radiol. 29* 394-404, **2011**.
99. K. Kitajima, RC. Murphy, MA. Nathan, et al., Detection of recurrent prostate cancer after radical prostatectomy: comparison of 11C-choline PET/CT with pelvic multiparametric MR imaging with endorectal coil, *J. Nucl. Med. 55* 223-32, **2014**
100. S. Fanti, S. Minozzi, P. Castellucci, et al., PET/CT with (11)C-choline for evaluation of prostate cancer patients with biochemical recurrence: meta-analysis and critical review of available data, *Eur. J. Nucl. Med. Mol. Imaging 43* 55-69, **2016**

101. C. Fuccio, P. Castellucci, R. Schiavina, et al., Role of 11C-choline PET/CT in the re-staging of prostate cancer patients with biochemical relapse and negative results at bone scintigraphy, *Eur. J. Radiol. 81* e893-6 **2012**.
102. C. Fuccio, P. Castellucci, R. Schiavina, et al., Role of 11C-choline PET/CT in the restaging of prostate cancer patients showing a single lesion on bone scintigraphy, *Ann. Nucl. Med. 24* 485-92., **2010**.
103. DK. Osmonov, D. Heimann, I. Janssen, et al., Sensitivity and specificity of PET/CT regarding the detection of lymph node metastases in prostate cancer recurrence, *Springer Plus. 3* 340, **2014**.
104. NM. Passoni, N. Suardi, F. Abdollah, et al., Utility of [11C]choline PET/CT in guiding lesion-targeted salvage therapies in patients with prostate cancer recurrence localized to a single lymph node at imaging: results from a pathologically validated series, *Urol. Oncol. 32* e9–16, **2014**.
105. JA. Richter, M. Rodriguez, J. Rioja, et al., Dual tracer 11C-choline and FDG-PET in the diagnosis of biochemical prostate cancer relapse after radical treatment, *Mol. Imaging Biol. 12* 210–7, **2010**.
106. V. Scattoni, M. Picchio, N. Suardi, et al., Detection of lymph-node metastases with integrated [11C] choline PET/CT in patients with PSA failure after radical retropubic prostatectomy: results confirmed by open pelvicretroperitoneal lymphadenectomy, *Eur. Urol. 52* 423–9, **2007**.
107. D. Tilki, O. Reich, A. Graser, et al., 18F-Fluoroethylcholine PET/CT identifies lymph node metastasis in patients with prostate-specific antigen failure after radical prostatectomy but underestimates its extent. , *Eur. Urol. 63* 792–6, **2013**.
108. F. Alongi, T. Comito, E. Villa, et al., What is the role of [11C]choline PET/CT in decision making strategy before post-operative salvage radiation therapy in prostate cancer patients?, *Acta Oncol. 53* 990–2, **2014**.
109. M. Souvatzoglou, BJ. Krause, A. Purschel, et al., Influence of (11)C-choline PET/CT on the treatment planning for salvage radiation therapy in patients with biochemical recurrence of prostate cancer, *Radiother. Oncol. 99* 193–200, **2011**.
110. F. Wurschmidt, C. Petersen, A. Wahl, et al., [18F] fluoroethylcholine-PET/CT imaging for radiation treatment planning of recurrent and primary prostate cancer with dose escalation to PET/CT-positive lymph nodes, *Radiat. Oncol. 6* 44, **2011**.
111. HC. Rischke, W. Schultze-Seemann, G. Wieser, et al., Adjuvant radiotherapy after salvage lymph node dissection because of nodal relapse of prostate cancer versus salvage lymph node dissection only, *Strahlenther Onkol. 191* 310–20, **2015**.
112. F. Ceci, P. Castellucci, T. Graziani, et al., 11C-choline PET/CT identifies osteoblastic and osteolytic lesions in patients with metastatic prostate cancer, *Clin. Nucl. Med. 40* e265–70, **2015**.
113. FDA approves 11C-choline for PET in prostate cancer, *J. Nucl. Med. 53* 11N, **2012**.
114. https://www.fda.gov/news-events/press-announcements/fda-approves-first-psma-targeted-pet-imaging-drug-men-prostate-cancer.
115. SC. Masters, AA. Hofling, A. Gorovets, L. Marzella, FDA Approves Ga 68 PSMA-11 for Prostate Cancer Imaging, *Int. J. Radiat. Oncol. Biol. Phys. 20* 357-6, **2021**.
116. IL. Alberts, SE. Seide, C. Mingels, et al., Comparing the diagnostic performance of radiotracers in recurrent prostate cancer: a systematic review and network meta-analysis, *Eur. J. Nucl. Med. Mol. Imaging Epublicaton online ahead of print.* Feb 6, **2021**.
117. C. Lawhn-Heath, A. Salavati, SC. Behr, et al., Prostate-specific Membrane Antigen PET in Prostate Cancer, *Radiology 299* 248-60, **2021**.
118. MS. Hofman, N. Lawrentschuk, RJ. Francis, et al., proPSMA Study Group Collaborators. Prostate-specific membrane antigen PET-CT in patients with high-risk prostate cancer before curative-intent surgery or radiotherapy (proPSMA): a prospective, randomised, multicentre study, *Lancet 395* 1208-16, **2020**.
119. JC. Lacal, T. Zimmerman, JM. Campos, Choline Kinase: An Unexpected Journey for a Precision Medicine Strategy in Human Diseases, *Pharmaceutics 13* 788-816, **2021**.
120. M. Cheng, ZM. Bhujwalla, K. Glunde, Targeting Phospholipid Metabolism in Cancer, *Front. Oncol. 6* 266-83, **2016**.
121. C. Aoyama, H. Liao, K. Ishidate, Structure and function of choline kinase isoforms in mammalian cells, *Prog. Lipid Res. 43* 266-81, **2004**.
122. D. Gallego-Ortega, A. Ramirez de Molina, MA. Ramos, et al., Differential role of human choline kinase alpha and beta enzymes in lipid metabolism: implications in cancer onset and treatment, *PLoS One 4* e7819, **2009**.
123. D. Mayer, D. Werner, Inhibition of choline kinase by selectively cytotoxic purinyl-6-histamine, *Biochem. Pharmacol. 23* 1227-30, **1974**.
124. M. Hamza, J. Lloveras, G. Ribbes, et al., An in vitro study of hemicholinium-3 on phospholipid metabolism of Krebs II ascites cells, *Biochem. Pharmacol. 32* 1893-7, **1983**.

125. J. Lloveras, M. Hamza, H. Chap, L. Douste-Blazy, Action of hemicholinium-3 on phospholipid metabolism in Krebs II ascites cells, *Biochem. Pharmacol. 34* 3987-93, **1985**.
126. MV. Miceli, LS. Kan, DA. Newsome, Phosphorus-31 nuclear magnetic resonance spectroscopy of human retinoblastoma cells: correlation with metabolic indices, *Biochim. Biophys. Acta 970* 262-9, **1988**.
127. GK. Radda, RD. Oberhaensli, DJ. Taylor, The biochemistry of human diseases as studied by 31P NMR in man and animal models, *Ann. NY Acad. Sci. 508* 300-8, **1987**.
128. JC. Lacal, Choline kinase: a novel target for antitumor drugs, *Drugs 4* 419–26, **2001**.
129. A. Ramírez de Molina, D. Gallego-Ortega, J. Sarmentero, et al., Choline kinase is a novel oncogene that potentiates RhoA-induced carcinogenesis, *Cancer Res. 65* 5647-53, **2005**.
130. A. Carnero, JC. Lacal, Activation of intracellular kinases in Xenopus oocytes by p21ras and phospholipases: a comparative study, *Mol. Cell Biol. 15* 1094-101, **1995**.
131. R. Hernández-Alcoceba, L. Saniger, J. Campos, et al., Choline kinase inhibitors as a novel approach for antiproliferative drug design, *Oncogene 15* 2289-301, **1997**.
132. B. Jiménez, L. del Peso, S. Montaner, et al., Generation of phosphorylcholine as an essential event in the activation of Raf-1 and MAP-kinases in growth factors-induced mitogenic stimulation, *J. Cell Biochem. 57* 141-9, **1995**.
133. JC. Lacal, Diacylglycerol production in Xenopus laevis oocytes after microinjection of p21ras proteins is a consequence of activation of phosphatidylcholine metabolism, *Mol. Cell Biol. 10* 333-40, **1990**.
134. JC. Lacal, J. Moscat, SA. Aaronson, Novel source of 1,2-diacylglycerol elevated in cells transformed by Ha-ras oncogene, *Nature Reviews Cancer 330* 269-72, **1987**.
135. IG. Macara, Elevated phosphocholine concentration in ras-transformed NIH 3T3 cells arises from increased choline kinase activity, not from phosphatidylcholine breakdown, *Mol. Cell Biol. 9* 325-8, **1989**.
136. D. Teegarden, EJ. Taparowsky, C. Kent, Altered phosphatidylcholine metabolism in C3H10T1/2 cells transfected with the Harvey-ras oncogene, *J. Biol. Chem. 265* 6042-7, **1990**.
137. GB. Ansell, SG. Spanner, The inhibition of brain choline kinase by hemicholinium-3, *J. Neurochem. 22* 1153-5, **1974**.
138. JG. Cannon, Structure-activity aspects of hemicholinium-3 (HC-3) and its analogs and congeners, *Med. Res. Rev. 14* 505-31, **1994**
139. R. Hernández-Alcoceba, F. Fernández, JC. Lacal, In vivo antitumor activity of choline kinase inhibitors: a novel target for anticancer drug discovery, *Cancer Res. 59* 3112-8, **1999**.
140. NM. Al-Saffar, H. Troy, A. Ramírez de Molina, et al., Noninvasive magnetic resonance spectroscopic pharmacodynamic markers of the choline kinase inhibitor MN58b in human carcinoma models, *Cancer Res. 66* 427-34, **2006**.
141. M. Kumar, SP. Arlauckas, S. Saksena, et al., Magnetic resonance spectroscopy for detection of choline kinase inhibition in the treatment of brain tumors, *Mol. Cancer Ther. 14* 899-908, **2015**.
142. R. Sánchez-Martín, JM. Campos, A. Conejo-García, et al., Symmetrical bis-quinolinium compounds: new human choline kinase inhibitors with antiproliferative activity against the HT-29 cell line, *J. Med. Chem. 48* 3354-63, **2005**
143. Study of Intravenous TCD-717 in Patients With Advanced Solid Tumors, Phase I trial of TCD-717, *https://.gov/ct2/show/NCT01215864*.
144. JC. Lacal, JM. Campos, Preclinical characterization of RSM-932A, a novel anticancer drug targeting the human choline kinase alpha, an enzyme involved in increased lipid metabolism of cancer cells, *Mol. Cancer Ther. 14* 31-9, **2015**.
145. SL. Kall, EJ. Delikatny, A. Lavie, Identification of a Unique Inhibitor-Binding Site on Choline Kinase α, *Biochemistry 57* 1316-25, **2018**.
146. SC. Falcon, CS. Hudson, Y. Huang, et al., A non-catalytic role of choline kinase alpha is important in promoting cancer cell survival, *Oncogenesis 2* e38, **2013**.
147. N. Mori, F. Wildes, S. Kakkad, et al., Choline kinase-α protein and phosphatidylcholine but not phosphocholine are required for breast cancer cell survival, *NMR Biomed. 28* 1697-706, **2015**.
148. DI. Hoult, SJ. Busby, DG. Gadian, GK. Radda, RE. Richards, PJ. Seeley, Observation of tissue metabolites using 31P nuclear magnetic resonance, *Nature Reviews Cancer 252* 285-7, **1974**.
149. PC. Lauterbur, Image Formation by Induced Local Interactions: Examples Employing Nuclear Magnetic Resonance, *Nature Reviews Cancer 242* 190–91, **1973**.
150. ID. Cresshull, RE. Gordon, PE. Hanley, et al., Localisation of Metabolites in Animal and Human Tissues Using 31P Topical Magnetic Resonance, *Bull. Magn. Res. 2* 426, **1980**.

151. JR. Griffiths, E. Cady, RH. Edwards, et al., 31P-NMR studies of a human tumour in situ, *Lancet 1* 1435-6, **1983**.
152. JM. Maris, AE. Evans, AC. McLaughlin, et al., 31P nuclear magnetic resonance spectroscopic investigation of human neuroblastoma in situ, *New Engl. J. Med. 312* 1500-5, **1985**
153. H. Bruhn, J. Frahm, ML. Gyngell, et al., Noninvasive differentiation of tumors with use of localized H-1 MR spectroscopy in vivo: initial experience in patients with cerebral tumors, *Radiology 172* 541-8, **1989**.
154. AA. Maudsley, OC. Andronesi, PB. Barker, et al., Advanced magnetic resonance spectroscopic neuroimaging: Experts' consensus recommendations, *NMR Biomed. 34* 1-22, **2021**.
155. AC. Westphalen, Lost in translation: lessons learned from the "demise" of MRSI of the prostate, *Abdom. Radiol. (NY) 44* 3185-87, **2019**.
156. R. Faghihi, B. Zeinali-Rafsanjani, MA. Mosleh-Shirazi, et al., Magnetic Resonance Spectroscopy and its Clinical Applications: A Review, *J. Med. Imaging Radiat. Sci. 48* 233-53, **2017**.
157. https://clinicaltrials.gov/.
158. PA. Bottomley, WA. Edelstein, TH. Foster, WA. Adams, In vivo solvent-suppressed localized hydrogen nuclear magnetic resonance spectroscopy: a window to metabolism?, *Proc. Natl. Acad. Sci. USA 82* 2148-52, **1985**.
159. J. Frahm, Localized Proton Spectroscopy using stimulated echoes, *J. Magn. Reson. 72* 502– 08, **1987**.
160. J. Frahm, H. Bruhn, ML. Gyngell, et al., Localized high-resolution proton NMR spectroscopy using stimulated echoes: initial applications to human brain in vivo, *Magn. Reson. Med.* 79-93, **1989**.
161. PR. Luyten, AJ. Marien, W. Heindel, et al., Metabolic imaging of patients with intracranial tumors: H-1 MR spectroscopic imaging and PET, *Radiology 176* 791-9, **1990**.
162. C. Choi, SK. Ganji, RJ. DeBerardinis, et al., 2-hydroxyglutarate detection by magnetic resonance spectroscopy in IDH-mutated patients with gliomas, *Nature Med. 18* 624-9, **2012**.
163. JH. Langkowski, J. Wieland, H. Bomsdorf, et al., Pre-operative localized in vivo proton spectroscopy in cerebral tumors at 4.0 Tesla--first results, *Magn. Reson. Imaging 7* 547-55, **1989**.
164. R. Hourani, A. Horská, S. Albayram, et al., Proton magnetic resonance spectroscopic imaging to differentiate between nonneoplastic lesions and brain tumors in children, *J. Magn. Reson. Imaging 23* 99-107, **2006**
165. P.B. Barker, N-Acetyl Aspartate—A Neuronal Marker?, *Ann. Neurol. 49* 423-24., **2001**.
166. TR. Brown, BM. Kincaid, K. Ugurbil, NMR chemical shift imaging in three dimensions, *Proc. Natl. Acad. Sci. USA 79* 3523-6, **1982**
167. Jack S. Cohen, Jerzy W. Jaroszewski, Ofer Kaplan, Jesus Ruiz-Cabello, Steven W. Collier, A history of biological applications of NMR spectroscopy, *Progress Nucl. Magn. Reson. Spect. 28* 53-85, **1995**.
168. J. Zhong, V. Huang, SS. Gurbani, et al., 3D whole-brain metabolite imaging to improve characterization of low-to-intermediate grade gliomas, *J. Neurooncol. 153* 303-11, **2021**.
169. W. Negendank, Studies of human tumors by MRS: a review, *NMR Biomed. 5* 303-24, **1992**.
170. FA. Howe, SJ. Barton, SA. Cudlip, et al., Metabolic profiles of human brain tumors using quantitative in vivo 1H magnetic resonance spectroscopy, *Magn. Reson. Med. 49* 223-32, **2003**.
171. JS. Taylor, JW. Langston, WE. Reddick, t al., Clinical value of proton magnetic resonance spectroscopy for differentiating recurrent or residual brain tumor from delayed cerebral necrosis, *Int. J. Radiat. Oncol. Biol. Phys. 36* 1251-61, **1996**.
172. MC. Preul, Z. Caramanos, DL. Collins, et al., Accurate, noninvasive diagnosis of human brain tumors by using proton magnetic resonance spectroscopy, *Nature Med. 2* 323-5, **1996**.
173. MC. Preul, Z. Caramanos, R. Leblanc, et al., Using pattern analysis of in vivo proton MRSI data to improve the diagnosis and surgical management of patients with brain tumors, *NMR Biomed. 11* 192-200, **1998**.
174. FS. De Edelenyi, C. Rubin, F. Estève, et al., A new approach for analyzing proton magnetic resonance spectroscopic images of brain tumors: nosologic images, *Nature Med. 6* 1287-9, **2000**.
175. AR. Tate, JR. Griffiths, I. Martínez-Pérez, et al., Towards a method for automated classification of 1H MRS spectra from brain tumours, *NMR Biomed. 11* 177-91, **1998**.
176. AR. Tate, C. Majós, A. Moreno, et al., Automated classification of short echo time in in vivo 1H brain tumor spectra: a multicenter study, *Magn. Reson. Med. 49* 29-36, **2003**.
177. M. Julià-Sapé, JR. Griffiths, AR. Tate, et al., Classification of brain tumours from MR spectra: the INTERPRET collaboration and its outcomes, *NMR Biomed. 28* 1772-87, **2015**.
178. AR. Tate, J. Underwood, DM. Acosta, et al., Development of a decision support system for diagnosis and grading of brain tumours using in vivo magnet-

ic resonance single voxel spectra, *NMR Biomed. 19* 411-34, **2006**.
179. A. Horská, PB. Barker, Imaging of brain tumors: MR spectroscopy and metabolic imaging, *Neuroimaging Clin. N. Am. 20* 293-310, **2010**.
180. http://www.aetna.com/cpb/medical/data/200_299/0202.html.
181. https://www.uhcprovider.com/content/dam/provider/docs/public/policies/signaturevalue-mmg/magnetic-resonance-spectroscopy-sv.pdf.
182. AM. Omuro, CC. Leite, K. Mokhtari, JY. Delattre, Pitfalls in the diagnosis of brain tumours, *Lancet Neurol. 5* 937-48, **2006**.
183. R. Hourani, LJ. Brant, T. Rizk, et al., Can proton MR spectroscopic and perfusion imaging differentiate between neoplastic and nonneoplastic brain lesions in adults?, *Am. J. Neuroradiol. 29* 366-72, **2008**.
184. WB. Pope, Brain metastases: neuroimaging, *Handbk. Clin. Neurol. 149* 89-112, **2018**.
185. H. Ishimaru, M. Morikawa, S. Iwanaga, et al., Differentiation between high-grade glioma and metastatic brain tumor using single-voxel proton MR spectroscopy, *Eur. Radiol. 11* 1784-91, **2001**.
186. IC. Chiang, YT. Kuo, CY. Lu, et al., Distinction between high-grade gliomas and solitary metastases using peritumoral 3-T magnetic resonance spectroscopy, diffusion, and perfusion imagings, *Neuroradiology 46* 619-27, **2004**.
187. S. Chawla, Y. Zhang, S. Wang, et al., Proton magnetic resonance spectroscopy in differentiating glioblastomas from primary cerebral lymphomas and brain metastases, *J. Comput. Assist. Tomogr. 34* 836-41, **2010**.
188. G. Fan, B. Sun, Z. Wu, Q. Guo, Y. Guo, In vivo single-voxel proton MR spectroscopy in the differentiation of high-grade gliomas and solitary metastases, *Clin Radiol. 59* 77-85, **2004.**
189. A. Server, R. Josefsen, B. Kulle, et al., Proton magnetic resonance spectroscopy in the distinction of high-grade cerebral gliomas from single metastatic brain tumors, *Acta Radiol.* 316-25, **2010**.
190. LA. Brandao, M. Castillo, Lymphomas-Part 1, *Neuroimaging Clin. N. Am. 26* 511–36, **201**???.
191. H. Nagashima, T. Sasayama, K. Tanaka, et al., Myo-inositol concentration in MR spectroscopy for differentiating high grade glioma from primary central nervous system lymphoma, *J. Neurooncol. 136* 317–26, **2018**.
192. A. Vallee, C. Guillevin, M. Wager, et al., Added Value of Spectroscopy to Perfusion MRI in the Differential Diagnostic Performance of Common Malignant Brain Tumors, *Am. J. Neuroradiol. 39* 1423–31, **2018**.
193. SS. Lu, SJ. Kim, HS. Kim, et al., Utility of proton MR spectroscopy for differentiating typical and atypical primary central nervous system lymphomas from tumefactive demyelinating lesions, *Am. J. Neuroradiol. 35* 270–77, **2014**.
194. R Ikeguchi, Y Shimizu, K Abe, et al., Proton magnetic resonance spectroscopy differentiates tumefactive demyelinating lesions from gliomas, *Mult. Scler. Relat. Disord. 26* 77–84, **2018**.
195. M. Garg, RK. Gupta, MR Spectroscopy in intracranial infection, in *Clinical MR Neuroimaging: Diffusion, Perfusion and Spectroscopy*, ed. by J. Gillard, A. Waldman, P. Barker, Cambridge University Press, Cambridge, UK:, pp. 380–406, **2004**.
196. C. Remy, S. Grand, ES. Lai, et al., 1H MRS of human brain abscesses in vivo and in vitro, *Magn. Reson. Med. 34* 508–14, **1995**.
197. D. Pal, A. Bhattacharyya, M. Husain, et al., In vivo proton MR spectroscopy evaluation of pyogenic brain abscesses: a report of 194 cases, *Am. J. Neuroradiol. 31* 360–66, **2010**.
198. O. Speck, T. Thiel, J. Hennig, Grading and therapy monitoring of astrocytomas with 1H-spectroscopy: preliminary study, *Anticancer Res. 16* 1581-5, **1996.**
199. MC. Preul, R. Leblanc, Z. Caramanos, et al., Magnetic resonance spectroscopy guided brain tumor resection: differentiation between recurrent glioma and radiation change in two diagnostically difficult cases, *Can. J. Neurol. Sci.* 13-22, **1998**.
200. PE. Ricci, A. Pitt, PJ. Keller, et al., Effect of voxel position on single-voxel MR spectroscopy findings, *Am. J. Neuroradiol. 21* 367-74., **2000**.
201. C. Senft, E. Hattingen, U. Pilatus, et al., Diagnostic value of proton magnetic resonance spectroscopy in the noninvasive grading of solid gliomas: comparison of maximum and mean choline values, *Neurosurgery* 908-13, **2009**.
202. S. Chawla, S. Wang, RL. Wolf, et al., Arterial spin-labeling and MR spectroscopy in the differentiation of gliomas, *Am J Neuroradiol* 1683–89, **2007**.
203. M. Bulik, R. Jancalek, J. Vanicek, et al., Potential of MR spectroscopy for assessment of glioma grading, *Clin. Neurol. Neurosurg. 115* 146–53, **2013**.
204. Q. Wang, H. Zhang, J. Zhang, et al., The diagnostic performance of magnetic resonance spectroscopy in differentiating high-from low-grade gliomas: A systematic review and meta-analysis, *Eur Radiol. 26* 2670–84, **2016**.
205. A. Arslanoglu, D. Bonekamp, PB. Barker, et al., Quantitative proton MR spectroscopic imaging of

the mesial temporal lobe, *J. Magn. Reson. Imaging 20* 772–78, **2004**.
206. AA. Chan, A. Lau, A. Pirzkall, et al., Proton magnetic resonance spectroscopy imaging in the evaluation of patients undergoing gamma knife surgery for Grade IV glioma, *J. Neurosurg. 101* 467–75, **2004**.
207. FW. Crawford, IS. Khayal, C. McGue, et al., Relationship of pre-surgery metabolic and physiological MR imaging parameters to survival for patients with untreated GBM, *J. Neurooncol. 91* 337–51, **2009**.
208. S. Saraswathy, FW. Crawford, KR. Lamborn, et al., Evaluation of MR markers that predict survival in patients with newly diagnosed GBM prior to adjuvant therapy, *J. Neurooncol. 91* 69–81, **2009**.
209. KE Warren, JA Frank, JL Black, et al., Proton magnetic resonance spectroscopic imaging in children with recurrent primary brain tumors, *J. Clin. Oncol. 18* 1020–26, **2000**.
210. K. Parvez, A. Parvez, G. Zadeh, The diagnosis and treatment of pseudoprogression, radiation necrosis and brain tumor recurrence, *Int. J. Mol. Sci. 15* 11832–46, **2014**.
211. A. Siu, JJ. Wind, JB. Iorgulescu, et al., Radiation necrosis following treatment of high grade glioma--a review of the literature and current understanding, *Acta Neurochir. (Wien) 154* 191–201, **2012**.
212. M. Chernov, M. Hayashi, M. Izawa, et al., Differentiation of the radiation-induced necrosis and tumor recurrence after gamma knife radiosurgery for brain metastases: importance of multi-voxel proton MRS, *Minim. Invasive Neurosurg. 48* 228-34, **2005**.
213. MF. Chernov, M. Hayashi, M. Izawa, et al., Multivoxel proton MRS for differentiation of radiation-induced necrosis and tumor recurrence after gamma knife radiosurgery for brain metastases, *Brain Tumor Pathol. 23* 19–27, **2006**.
214. LL. Wald, SJ. Nelson, MR. Day, et al., Serial proton magnetic resonance spectroscopy imaging of glioblastoma multiforme after brachytherapy, *J. Neurosurg. 87* 525–34, **1997**.
215. EA. Smith, RC. Carlos, LR. Junck, et al., Developing a clinical decision model: MR spectroscopy to differentiate between recurrent tumor and radiation change in patients with new contrast-enhancing lesions, *Am. J. Roentgenol. 192* W45–W52, **2009**.
216. X. Li, DB. Vigneron, S. Cha, et al., Relationship of MR-derived lactate, mobile lipids, and relative blood volume for gliomas in vivo, *Am. J. Neuroradiol. 26* 760–69, **2005**.
217. JP. Rock, D. Hearshen, L. Scarpace, et al., Correlations between magnetic resonance spectroscopy and image-guided histopathology, with special attention to radiation necrosis, *Neurosurgery 51* 912–19, **2002**.
218. T. Nakajima, T. Kumabe, M. Kanamori, et al., Differential diagnosis between radiation necrosis and glioma progression using sequential proton magnetic resonance spectroscopy and methionine positron emission tomography, *Neurol. Med. Chir. (Tokyo) 49* 394–401, **2009**.
219. H. Zhang, L. Ma, Q. Wang, et al., Role of magnetic resonance spectroscopy for the differentiation of recurrent glioma from radiation necrosis: a systematic review and meta-analysis, *Eur. J. Radiol. 83* 2181–89, **2014**.
220. BRJ. van Dijken, PJ. van Laar, GA. Holtman , A. van der Hoorn, Diagnostic accuracy of magnetic resonance imaging techniques for treatment response evaluation in patients with high-grade glioma, a systematic review and meta-analysis, *Eur. Radiol. 27* 4129–44, **2017**.
221. A. Di Costanzo, T. Scarabino, F. Trojsi, et al., Multiparametric 3T MR approach to the assessment of cerebral gliomas: tumor extent and malignancy, *Neuroradiology 48* 622–31, **2006**.
222. EJ. Hermann, E. Hattingen, JK. Krauss, et al., Stereotactic biopsy in gliomas guided by 3-tesla 1H–chemical-shift imaging of choline, *Stereotact. Funct. Neurosurg. 86* 300–7, **2008.**
223. JS. Cordova, HK. Shu, Z. Liang, et al., Whole-brain spectroscopic MRI biomarkers identify infiltrating margins in glioblastoma patients, *Neuro. Oncol. 18* 1180–89, **2016**.
224. JS. Cordova, S. Kandula, S. Gurbani, et al., Simulating the Effect of Spectroscopic MRI as a Metric for Radiation Therapy Planning in Patients with Glioblastoma, *Tomography 2* 366–73, **2016**.
225. S. Ken, L. Vieillevigne, X. Franceries, et al., Integration method of 3D MR spectroscopy into treatment planning system for glioblastoma IMRT dose painting with integrated simultaneous boost, *Radiat. Oncol. 8* 1, **2013**.
226. https://clinicaltrials.gov/ct2/show/NCT03137888
227. George Shu Hui-Kuo, Eric Albert Mellon, Lawrence Kleinberg, et al., A multisite clinical trial of spectroscopic MRI-guided radiation dose escalation for newly-diagnosed glioblastomas, *J. Clin.Oncol. 39:15 suppl* 2018, **2021**.
228. M Wilson, O Andronesi, PB Barker, et al.. Methodological consensus on clinical proton MRS of the brain: Review and recommendations., *Magn. Reson. Med. 82* 527-50, **2019**.
229. https://www.gehealthcare.com/article/15t-compared-to-30t-mri-scanners.

230. A. Nowogrodzki, The world's strongest MRI machines are pushing human imaging to new limits, *Nature Med. 563* 24-26, **2018**.
231. M.A. Thomas, P. Narayan, J. Kurhanewicz, et al., 1H MR spectroscopy of normal and malignant human prostates in Vivo, , *Journal of Magnetic Resonance 87* 610-19, **1990**.
232. J. Kurhanewicz, A. Thomas, P. Jajodia, et al., 31P spectroscopy of the human prostate gland in vivo using a transrectal probe., *Magn. Reson. Med. 22* 404-13, **1991**
233. J. Kurhanewicz, DB. Vigneron, H. Hricak, et al., Three-dimensional H-1 MR spectroscopic imaging of the in situ human prostate with high (0.24-0.7-cm3) spatial resolution, *Radiology 198* 795-805, **1996**.
234. JO. Barentsz, J. Richenberg, R. Clements, et al., European Society of Urogenital Radiology. ESUR prostate MR guidelines 2012, *Eur. Radiol. 22* 746-57, **2012**.
235. A. Stabile, F. Giganti, AB. Rosenkrantz, et al., Multiparametric MRI for prostate cancer diagnosis: current status and future directions, *Nat. Rev. Urol. 17* 41-61, **2020**
236. F. Giganti, AB. Rosenkrantz, G. Villeirs, et al., The Evolution of MRI of the Prostate: The Past, the Present, and the Future, *Am. J. Roentgenol. 213* 384-96, **2019**
237. PE. Sijens, HK. Wijrdeman, MA. Moerland, et al., Human breast cancer in vivo: H-1 and P-31 MR spectroscopy at 1.5 T, *Radiology 169* 615-20, **1988**.
238. J. Glaholm, M. O. Leach, D. J. Collins, et al., In-vivo 31P magnetic resonance spectroscopy for monitoring tumour response in breast cancer, *Lancet 333* 1326–27 **1989**.
239. T. C. Ng, S. Grundfest, S. Vijayakumar, et al., Therapeutic response of breast carcinoma monitored by 31P MRS in situ, *Magn. Reson. Med. 10* 125–34, **1989**.
240. MO. Leach, M. Verrill, J. Glaholm, et al., Measurements of human breast cancer using magnetic resonance spectroscopy: a review of clinical measurements and a report of localized 31P measurements of response to treatment, *NMR Biomed. 11* 314-40, **1998**.
241. T. A. Smith, J. Glaholm, M. O. Leach, et al., A comparison of in vivo and in vitro 31P NMR spectra from human breast tumours: variations in phospholipid metabolism, *Br. J. Cancer 63* 514–16, **1991**.
242. R. Katz-Brull, PT. Lavin, RE. Lenkinski, Clinical utility of proton magnetic resonance spectroscopy in characterizing breast lesions, *J. Natl. Cancer Inst. 94* 1197-203, **2002**.
243. GL Menezes, FM. Knuttel, BL. Stehouwer, et al., Magnetic resonance imaging in breast cancer: A literature review and future perspectives, *World J. Clin. Oncol. 10* 61-70, **2014**.
244. R. Fardanesh, MA. Marino, D. Avendano, et al., Proton MR spectroscopy in the breast: Technical innovations and clinical applications, *J. Magn. Reson. Imaging 50* 1033-46, **2019**
245. T. Shah, B. Krishnamachary, F. Wildes, et al., Molecular causes of elevated phosphoethanolamine in breast and pancreatic cancer cells, *NMR Biomed. 31* e3936, **2018**.
246. AGV. Bitencourt, J. Goldberg, K. Pinker, SB. Thakur, Clinical applications of breast cancer metabolomics using high-resolution magic angle spinning proton magnetic resonance spectroscopy (HRMAS 1H MRS): systematic scoping review, *Metabolomics 15* 148, **2019**.
247. LA. Vandergrift, EA. Decelle, J. Kurth, et al., Metabolomic Prediction of Human Prostate Cancer Aggressiveness: Magnetic Resonance Spectroscopy of Histologically Benign Tissue, *Sci. Rep. 8* 4997, **2018**.
248. M. Donadon, E. Lopci, J. Galvanin, et al., Prognostic Value of Metabolic Imaging Data of 11C-choline PET/CT in Patients Undergoing Hepatectomy for Hepatocellular Carcinoma, *Cancers 13* 472, **2021**.
249. G. Treglia, A. Piccardo, A. Imperiale, et al., Diagnostic performance of choline PET for detection of hyperfunctioning parathyroid glands in hyperparathyroidism: a systematic review and meta-analysis, *Eur. J. Nucl. Med. Mol. Imaging 46* 751-65, **2019**.